RE: A point-to-point response to reviewers' comments

"Secondary OH reactions of aromatics-derived oxygenated organic molecules lead to plentiful highly oxygenated organic molecules within an intraday OH exposure" by Yuwei Wang, Chuang Li, Ying Zhang, Yueyang Li, Gan Yang, Xueyan Yang, Yizhen Wu, Lei Yao, Hefeng Zhang, Lin Wang (egusphere-2023-1702)

Dear Dr. Liggio,

We are very grateful for the comments from both reviewers and the revision opportunity you offered to improve our work. To address the concerns raised by the reviewer, extra experiments under atmospheric relevant OH concentrations ([OH]) have been conducted to make comparisons between results from high and low [OH] experiments. Nevertheless, this manuscript does not suggest that the product distributions are identical between ambient conditions and laboratory experiments, but is meant to elucidate the potential or ability of OOMs to generate more diverse HOMs if they survive for a long period of time.

A point-to-point response to the comments, which are repeated in *italic*, is given below.

We are looking forward to your decision at your earliest convenience.

Best regards,

Lin Wang
Fudan University
lin_wang@fudan.edu.cn

Reviewer #1*: I thank the Authors for considering my comments on the work. While I do feel that several of my concerns were not really answered, I nevertheless appreciate the invested effort.*

I am still not convinced that PAM type OFR setups could be used to study atmospheric relevant chemical mechanisms due to their high oxidant load conditions, and the usage of high doses of UV light, especially in connection to studying aromatic compound oxidation reactions. PAM type setups are apparently useful for deriving emission regulations as it is possible to, at least to an extent, estimate the amount of SOA produced during a long atmospheric processing time. These systems, by design, deviate from ambient concentration ranges, and thus are generally unsuited to study ambient relevant reaction mechanisms.

R1. We thank the reviewer for his comments. To address concerns raised by the reviewer on the high OH concentrations ([OH]) used in our experiments, extra experiments under atmospheric relevant $OH/HO_2/RO_2$ radical concentrations were conducted. Results in the new experiments show that the multi-generation OH oxidation and the corresponding products are manifest at atmospheric relevant [OH] (~10^7 molecule cm^{-3}), even when the OH exposure is as low as 5.86×10^8 molecule cm^{-3} s. The comparison between oxidation products detected in the low [OH] and high [OH] laboratory experiments show a shift in the relative abundance toward compounds with more hydrogen atoms under high [OH] experiments, which confirms that these compounds are strongly related to the accelerated RO_2 termination and multi-generation OH oxidation.

We agree with the reviewer that the conclusion of our high [OH] experiments is limited to show the potential or ability of aromatics-derived, stabilized OH oxidation products to generate more diverse HOM products by the re-initiation of OH oxidation, i.e., the existence of the sub-sequential oxidation of stabilized oxidation products. If the survival time of a specific OOM product permits, the re-initiation of its OH oxidation, i.e., OOM + OH → new-RO_2, can be deduced/confirmed with the detection of compounds with higher hydrogen contents or nitrogen contents, i.e., lower double bond equivalence (DBE, calculated as $nC - \frac{nH+nN}{2} + 1$ where nC, nH, and nN stand for the number of carbon, hydrogen, and nitrogen atoms in a molecule, respectively). While supported to some extent by our new experiments with atmospheric relevant [OH], the existence of multi-generation OH oxidation of aromatics-derived OOMs under ambient conditions still necessitates further investigation, because of the significant variations in the detailed radical ratios, survival times of OOMs in the real atmosphere, and the exact atmospheric OH exposures under the diverse ambient conditions that cannot be captured solely through the current high [OH] experiments.

Nevertheless, this manuscript is meant to elucidate the potential formation pathways of HOMs, which are now supported by both high [OH] and atmospheric relevant [OH] experiments, if these HOMs were indeed formed and observed in ambient. The product distribution under ambient OH exposure, is not expected to be identical to that from OFR experiments with high [OH].

R 1.1. Methods of new experiments with atmospheric relevant [OH]

Seven extra experiments were conducted, four without NO_x and three with NO_x. Their experimental conditions are listed in Table R1. Hereafter, we refer to the previous series of experiments as 'the 1st-round experiments' and the new series as 'the 2nd-round experiments', respectively. The i^{th} experiment in the 1st-round experiments is labelled as 1-i and the one in the 2nd-round experiments as 2-i, where i stands for its serial number.

Table R1. Summary of the 2nd-round experiments.

	Initial concentration of 1,3,5-TMB (ppb)	O_3 concentration (ppb)*	NO concentration (ppb)	NO_2 concentration (ppb)	Estimated OH exposure based on the precursor consumption (× 10^8 molecule cm^{-3} s)
2-1	30.8	147	0	0	54.7
2-2	30.8	151	0	0	23.8
2-3	30.8	152	0	0	9.56
2-4	30.8	152	0	0	5.86
2-5	34.5	123	7.11	38	31.1
2-6	34.5	137	3.10	21	19.7
2-7	34.5	144	1.30	11	8.83

* O_3 concentrations were stable values measured after the lights were turned on.

The experimental methods for the 2nd-round experiments have been updated according to either the comments of the reviewer or the availability of instruments.

In the 2nd-round experiments, a Vocus CI-TOF (Towerk AG, Switzerland) equipped with a Vocus Aim inlet and the same nitrate-ion chemical ionization source as adopted in the 1st-round experiments was utilized to measure oxidation products, hereafter referred as nitrate CI-TOF. The nitrate CI-TOF is characterized with a flat transmission efficiency between m/z 60 Th and m/z 500 Th, as well as a mass resolution of 10000 at m/z 200 Th.

We kept the reactor a plug flow one, and kept the residence time the same as in 1st-round experiments. The sampling system of our PAM OFR has been updated with the help of Aerodyne Research Inc. We replaced the sampling port at the exit of PAM OFR, and the reaction products were sampled from the PAM OFR via a 30 cm-long Teflon tube with a 1/2 in. outer diameter (OD) to our nitrate CI-TOF in the 2nd-round experiments. The Vocus PTR and the ozone monitor were connected to the PAM OFR from a separate port via a 120 cm-long Teflon tube with a 1/4 in. OD.

The relative humidity was kept around 20%. The initial concentration of O_3, light intensities of 254 nm UV lamps, and the initial concentration of 1,3,5-TMB were all tuned down to make the conditions as close to the ambient as possible. An experiment with a lamp intensity and a concentration of O_3 lower than those in Exp. 2-4 was tested but very few convinced signals of HOMs were detected. In the NO_x experiments, due to the low (O^1D) in the PAM OFR, 2.5 slpm pure N_2O was utilized instead of the previous one (350 sccm), whereas the total flow was kept the same as in the 1st-round experiments. The average [OH] in the PAM OFR was estimated with PAM_chem_v8 constrained by the precursor consumption and measured O_3 concentrations. The autoxidation reaction rate of BPR has been updated to be 0.078 s^{-1} in the model as discussed below, and the results estimated by this model for the 1st-round experiments have also been updated using the updated autoxidation rate.

Contents in this part have been incorporated into **Section 2** and **the supplement** of the revised manuscript (version R2), which reads:

Line (146 - 174):

"**2 Methods**

OH-initiated oxidation of 1,3,5-TMB was investigated in a potential aerosol formation oxidation flow reactor (PAM OFR) system at T = 298 ± 1 K and a pressure of 1 atm (Lambe et al., 2015). Two series of experiments were conducted, one under high [OH] conditions and the other under low [OH] conditions.

Hereafter, we refer to the series of high [OH] experiments as 'the 1st-round experiments' and the low [OH] as 'the 2nd-round experiments', respectively. The *i*th experiment in the 1st-round experiments is labelled as 1-*i* and the one in the 2nd-round experiments as 2-*i*, where *i* stands for its serial number. The experimental settings in this study differed slightly from what were used previously (Wang et al., 2020b). In the 1st-round experiments, forty OH experiments without NO_x (Exp. 1-1 – 1-40) and twenty-eight experiments with NO_x (Exp. 1-41 – 1-68) were performed. Seven experiments were conducted in the 2nd-round, four without NO_x and three with NO_x. The experimental conditions are summarized in Table S1, including concentrations of the precursor, ozone, and NO and NO_2. The equivalent OH exposure in the OFR for each experiment was estimated according to the precursor consumption, also listed in Table S1. OH exposures in the OFR were in the range of $(5.2 – 48.7)\times10^9$ and $(0.6 – 5.5)\times10^9$ molecules cm^{-3} s in the 1st-round and 2nd-round experiments, respectively.

A home-made 1,3,5-TMB/N_2 cylinder was used as a stable gaseous precursor source in the experiments, from which the flow rate of 1,3,5-TMB/N_2 varied between 1 – 3 sccm (standard cubic centimeter per minute, standard to 0 °C, 1 atm), leading to 28.9 – 62.7 ppb of 1,3,5-TMB in the 1st-round experiments, and 30.8 or 34.5 ppb of 1,3,5-TMB in the 2nd-round experiments, respectively (Table S1). A total flow of 15 slpm (standard liters per minute, standard to 0 ° C, 1 atm) zero-gas generated by a zero-gas generator (model 737-13, Aadco Instruments Inc.), together with the 1,3,5-TMB/N_2 flow, was introduced into the OFR. The reaction time in both series of experiments was kept at around 53 s and the flow reactor was kept as a plug flow in both series. "

Line (179 - 181):

"through a separate ozone chamber, resulting in an initial ozone concentration of around 429 – 881 ppb in the OFR in the 1st-round experiments and 123 – 152 ppb in the 2nd-round experiments, respectively."

Line (208 - 222):

"For experiments with NO_x in the 1st-round experiments, 350 sccm N_2O …, while RH and irradiances were not changed. In the 2nd-round experiments, due to the lower (O^1D) in the PAM OFR, 2.5 slpm pure N_2O was utilized instead, whereas the total flow rate was kept the same as that in the 1st-round. We lowered the light intensity to obtain lower [OH] in the PAM OFR, which also resulted in fluctuations in the NO concentrations ([NO]) from 1.3 to 7.1 ppb and the NO_2 concentrations ([NO_2]) from 11 to 38 ppb."

Line (223 - 225):

"A nitrate CIMS (Ehn et al., 2014; Eisele and Tanner, 1993) and a Vocus PTR (Krechmer et al., 2018) were deployed at the exit of the OFR to measure the oxidation products of 1,3,5-TMB in the 1st-round experiments."

Line (227 - 228):

"The sample flow rate for the nitrate CIMS in the 1st round-experiments was 8 slpm through a Teflon tube"

Line (253 - 261):

"In the 2nd-round experiments, a Vocus CI-TOF (Towerk AG, Switzerland) equipped with a Vocus Aim inlet and the same nitrate-ion chemical ionization source as adopted in the 1st-round experiments was utilized to measure oxidation products, hereafter referred as nitrate CI-TOF. The nitrate CI-TOF was characterized

with a flat transmission efficiency between m/z 60 Th and m/z 500 Th, as well as a mass resolution of 10000 at m/z 200 Th.

In this series of experiments, the reaction products were sampled from the PAM OFR via a 30 cm-long Teflon tube with a 1/2 in. OD to our nitrate CI-TOF. The Vocus PTR and the ozone monitor were connected to the PAM OFR from a separate port via a 120 cm-long Teflon tube with a 1/4 in. OD."

Line (265 - 268):

"The initial concentrations of TMB utilized in both sets of experiments fluctuated slightly, which resulted from sample preparation processes and were more obvious in the 1st-round experiments. Therefore, in the discussion on the data of this series of experiments, we tried …"

and Line (315 - 321):

"For the 1st-round experiments, the input parameters of temperature, mean residence time, water vapor concentration, O_3 concentration, and the initial 1,3,5-TMB concentration are 25 °C, 53 s, 0.63%, 500 ppbv, and 50 ppbv, respectively, as measured directly. For the 2nd-round experiments, the input parameters of O_3 concentration and the initial 1,3,5-TMB concentration were updated as 150 ppb and 30.8 ppbv, respectively. In the NO_x experiments, the input flow rate of N_2O is 350 sccm in the 1st-round experiments and 2.5 slpm in the 2nd-round experiments, respectively."

R 1.2. Results of the low [OH] experiments

Given the larger sampling port, lower initial ozone concentrations, lower UV light intensities, and a better performance of mass spectrometer in this series of experiments, a number of new species were detected in the 2nd-round experiments, including three typical termination reaction products of BPR, i.e., $C_9H_{14}O_4$, $C_9H_{14}O_5$, and $C_9H_{13}NO_6$, and a number of low volatile compounds, e.g., $C_9H_xO_{11}$ (x = 12 - 15). The distributions of oxidation products detected by nitrate CI-TOF in Exp. 2-3, 2-4, and 2-7, representative low [OH] experiments, are displayed in Figure R1 (also as Figure 5 in the revised manuscript, version R2). The detailed molecular formula and their contributions to total HOMs signals are provided in the revised supplementary Table S6 and S7.

In addition, certain C9 and C18 HOMs with lower DBE than typical first-generation products predicted by MCM (Saunders et al., 2003) or reported by previous studies (Berndt et al., 2018), were detected in Exp. 2-3, 2-4, and 2-7, although [OH] in these experiments are much lower than those in the 1st-round experiments.

Observation of compounds with lower DBE in Exp. 2-3, 2-4, and 2-7 including HOM monomers with DBE lower than 3 and HOM dimers with DBE lower than 6, as well as monomer radicals with DBE lower than 3 including $C_9H_{15}O_m$· (m = 7 - 11) and $C_9H_{14}NO_9$·, proves the re-initiation of OH oxidation of the stabilized products in experiments with atmospheric relevant [OH]. All the stabilized products and radicals depicted in the proposed mechanisms (Scheme 2 and Scheme 3 in the previous reply and the previous version of manuscript, version R1) were detected in both Exp. 2-3 and Exp. 2-4, except for $C_9H_{15}O_9$· that was only detected in Exp. 2-3. This means that the proposed reaction pathways have already happened under atmospheric [OH] conditions with limited OH exposures. However, as we do not know the exact structures of these OOMs and radicals, the proposed reaction pathways are merely based on the chemical formulae detected by nitrate CIMS and nitrate CI-TOF and proposed according to the general mechanisms of OH addition reactions to the C=C bond. Other reaction pathways to generate these compounds or other isomers generated in these pathways are undoubtedly feasible.

A lot of compounds detected in the experiments without NO_x were not observed in counterpart

experiments with NO_x. We also did not detect decent signals of HOM dimers in the NO_x-present experiments in the 2nd-round experiments. This might come from the dominant significance of NO + RO_2 reactions (*R*8 - *R*9) after the introduction of NO_x into system, making signals of certain HOMs from other channels lower than the detection limit of the instrument. The proportions of other reaction channels decreased, and were reassigned to the NO channel, as evidenced by the fact that most of observed oxidation products were organonitrates, which is in an excellent agreement with the modeled channel proportions in **R 1.4** (Section 3.1 in the revised manuscript, version R2). The most significant nitrogen-containing compound was $C_9H_{13}NO_8$, whose formula matches the NO termination product of $C_9H_{13}O_7^{\cdot}$, i.e., autoxidation product of BPR. The second most abundant compound, $C_9H_{14}N_2O_{10}$ in our low [OH] experiments, was the most significant product in the high [OH] experiments in the presence of NO_x, whose formula matches the NO termination product of $C_9H_{14}NO_9^{\cdot}$, i.e., the RO_2 formed via an OH addition to $C_9H_{13}NO_6$, the NO termination product of BPR. All of the products and radicals mentioned above were observed in Exp. 2-7 with an atmospheric relevant [OH], as shown in Figure R1c (Figure 5c in the revised manuscript, version R2). From the perspective of molecular formula, $C_9H_{14}N_2O_{10}$ is also one of the most frequently observed multi-nitrogen-containing compound in polluted atmospheres, whose seasonal variations show a good correlation with [OH] (Guo et al., 2022; Yang et al., 2023).

We compared the difference in product distributions between Exp. 2-3 ([OH] = ~1.69×10^7 molecule cm^{-3}) and Exp. 2-1 ([OH] = ~1.03×10^8 molecule cm^{-3}), as well as between Exp. 2-3 and Exp. 1-12 ([OH] = ~8.47×10^8 molecule cm^{-3}) in Figure R2 (also as Figure 6 in the revised manuscript, version R2). The normalized abundance was obtained by normalizing all the products to the most abundant one in each experiment, i.e., $C_{18}H_{26}O_{10}$ in Exp. 2-1 and Exp. 2-3, and $C_9H_{14}O_7$ in Exp. 1-12. The changes in the normalized abundance were obtained by subtracting the normalized abundance in Exp. 2-1 from that in Exp. 2-3, and Exp. 1-12 from Exp. 2-3. As the [OH] and OH exposure increased, there was a noticeable rise in the relative abundance of more oxygenated compounds, which can be attributed to the more intensive proportion of multi-generation OH oxidation in high OH exposure experiments. This comparison demonstrates the capacity and potential of multi-generation OH oxidation to reduce DBE and elevate the oxygenated levels of oxidation products.

The changes in the normalized abundance of C9 and C18 do not correspond proportionally to the observed alterations in their absolute abundance. For example, the signals of $C_9H_xO_{11}$ (x = 12 - 15) products were actually higher in Exp. 2-1 than those in Exp. 2-3, but their normalized abundance is lower, which is due the faster increase in the signal of the most abundant compound $C_{18}H_{26}O_{10}$ in these experiments.

(a)

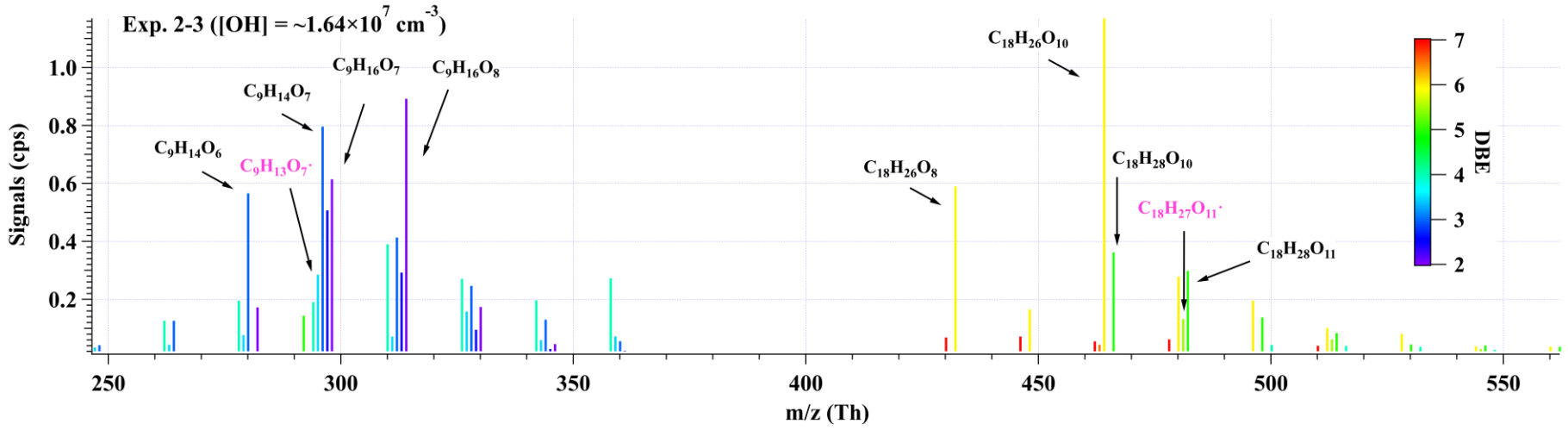
Exp. 2-3 ([OH] = ~1.64×10^7 cm^-3)
Signals (cps)
m/z (Th)
DBE
C9H14O6
C9H13O7·
C9H14O7
C9H16O7
C9H16O8
C18H26O8
C18H26O10
C18H28O10
C18H27O11·
C18H28O11

(b)

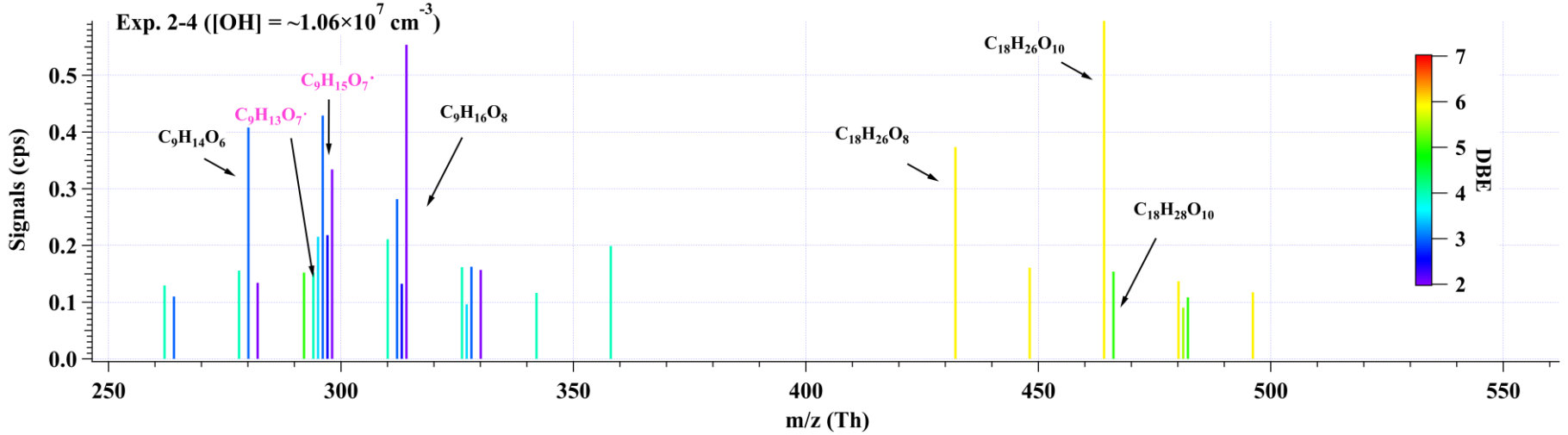
Exp. 2-4 ([OH] = ~1.06×10^7 cm^-3)
Signals (cps)
m/z (Th)
DBE
C9H14O6
C9H13O7·
C9H15O7·
C9H16O8
C18H26O8
C18H26O10
C18H28O10

(c)

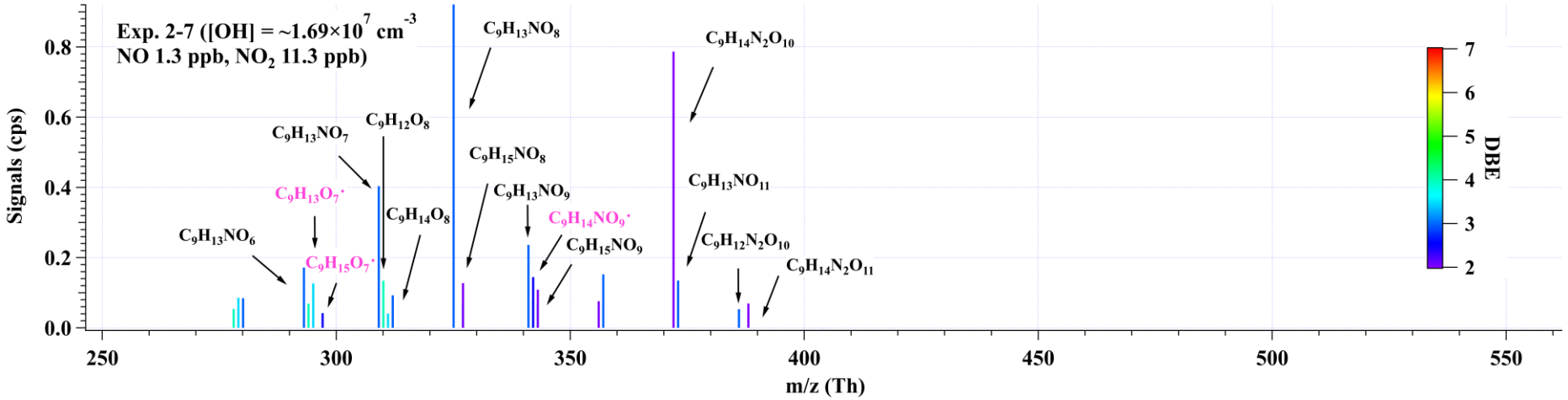

Figure R1. Distributions of C9 and C18 products detected by nitrate CI-TOF in (a) Exp. 2-3, (b) Exp. 2-4, and (c) Exp. 2-7. The reagent ion, NO_3^-, is omitted in the label for the molecular formula. Important radicals were labelled in pink. Note that no convinced signals of HOM dimers were observed in the 2nd-round experiments with NO_x.

(a)

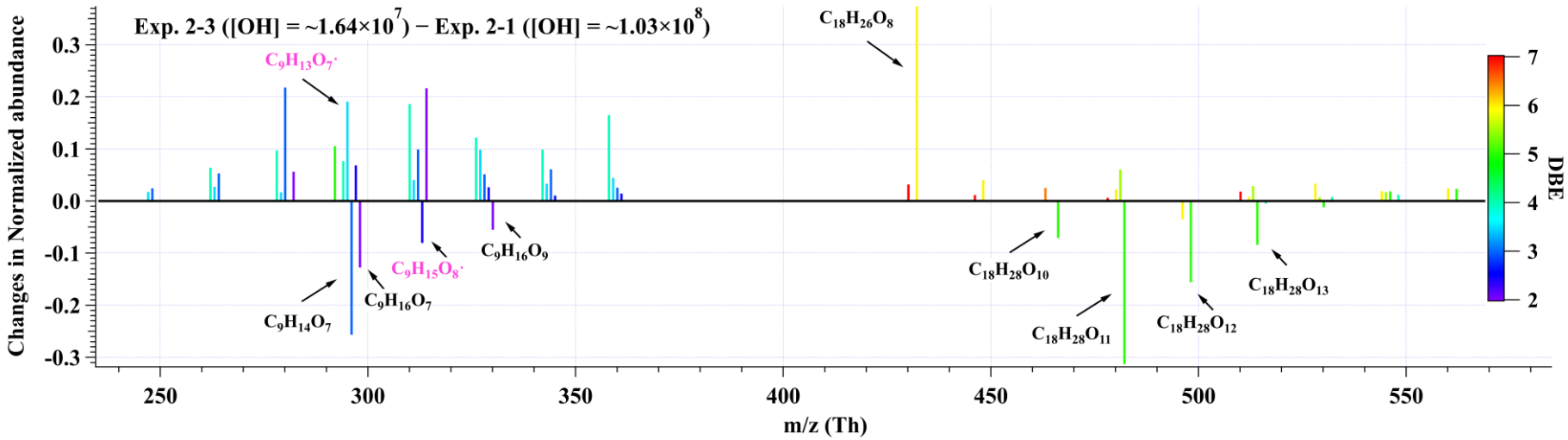
Exp. 2-3 ([OH] = ~1.64×10^7) − Exp. 2-1 ([OH] = ~1.03×10^8)
Changes in Normalized abundance
m/z (Th)
DBE
C9H13O7·
C9H14O7
C9H16O7
C9H15O8·
C9H16O9
C18H26O8
C18H28O10
C18H28O11
C18H28O12
C18H28O13

(b)

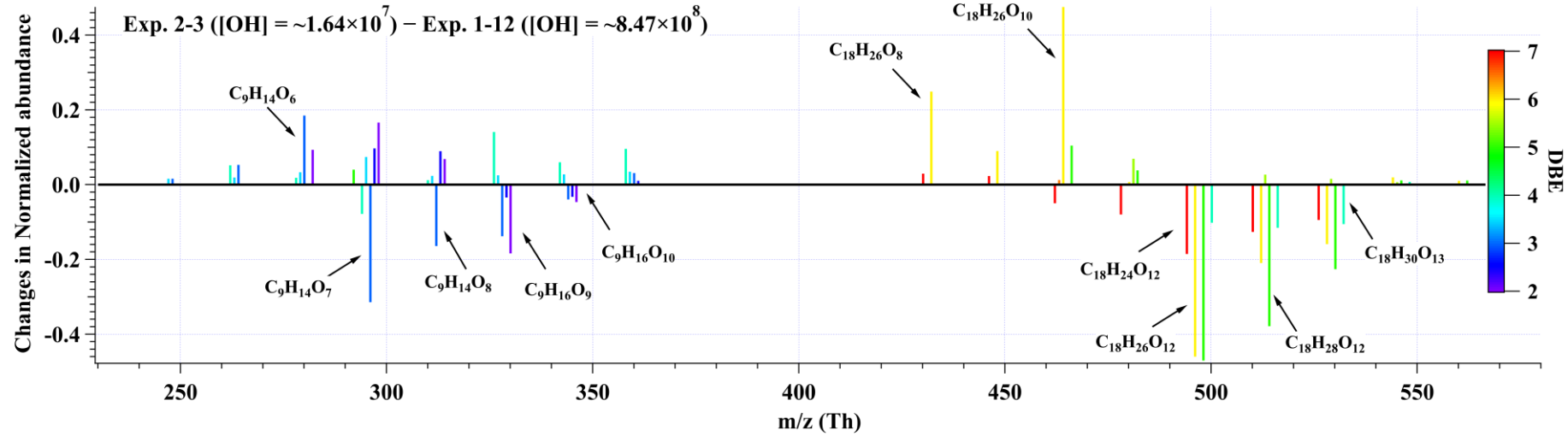
Exp. 2-3 ([OH] = ~1.64×10^7) − Exp. 1-12 ([OH] = ~8.47×10^8)
Changes in Normalized abundance
m/z (Th)
DBE
C9H14O6
C9H14O7
C9H14O8
C9H16O9
C9H16O10
C18H26O8
C18H26O10
C18H24O12
C18H26O12
C18H28O12
C18H30O13

Figure R2. The changes in the normalized abundance of C9 and C18 products observed by nitrate CI-TOF in (a) Exp. 2-3 relative to Exp. 2-1, and (b) Exp. 2-3 relative to Exp. 1-12. The reagent ion, NO_3^-, is omitted in the label. The normalized abundance was obtained by normalizing all the products to the most abundant one in each experiment, i.e., $C_{18}H_{26}O_{10}$ in Exp. 2-1 and Exp. 2-3, and $C_9H_{14}O_7$ in Exp. 1-12.

This part corresponds to the newly added **Section 3.3** in the revised manuscript (version R2).

We have revised our manuscript as:

Line (791 - 855):

3.3 Oxidation products in low [OH] experiments

Given the larger sampling port, lower initial ozone concentrations, lower UV light intensities, and a better performance of mass spectrometer in this series of low [OH] experiments, a number of new species were detected in the 2nd-round experiments, including three typical termination reaction products of BPR, i.e., $C_9H_{14}O_4$, $C_9H_{14}O_5$, and $C_9H_{13}NO_6$, and a number of low volatile compounds, e.g., $C_9H_xO_{11}$ (x = 12 - 15). The distributions of oxidation products detected by nitrate CI-TOF in Exp. 2-3, 2-4, and 2-7, representative low [OH] experiments, are displayed in Figure 5. The detailed molecular formula and their contributions to total HOMs signals are provided in Tables S6 and S7.

In addition, certain C9 and C18 HOMs with lower DBE than typical first-generation products predicted by MCM (Saunders et al., 2003) or reported by previous studies (Berndt et al., 2018b), were detected in Exp. 2-3, 2-4, and 2-7, although [OH] in these experiments are much lower than those in the 1st-round experiments.

Observation of compounds with lower DBE in Exp. 2-3, 2-4, and 2-7 including HOM monomers with DBE lower than 3 and HOM dimers with DBE lower than 6, as well as monomer radicals with DBE lower than 3 including $C_9H_{15}O_m^{\cdot}$ (m = 7 - 11) and $C_9H_{14}NO_9^{\cdot}$, proves the re-initiation of OH oxidation of the stabilized products in experiments with atmospheric relevant [OH]. All the stabilized products and radicals depicted in the proposed mechanisms (Scheme 2 and Scheme 3) were detected in both Exp. 2-3 and Exp. 2-4, except for $C_9H_{15}O_9^{\cdot}$ that was only detected in Exp. 2-3. This means that the proposed reaction pathways have already happened under atmospheric [OH] conditions with limited OH exposures. However, as we do not know the exact structures of these OOMs and radicals, the proposed reaction pathways are merely based on the chemical formulae detected by nitrate CIMS and nitrate CI-TOF and proposed according to the general mechanisms of OH addition reactions to the C=C bond. Other reaction pathways to generate these compounds or other isomers generated in these pathways are undoubtedly feasible.

A lot of compounds detected in the experiments without NO_x were not observed in counterpart experiments with NO_x. We also did not detect decent signals of HOM dimers in the NO_x-present experiments in the 2nd-round experiments. This might come from the dominant significance of NO + RO_2 reactions ($R8$ - $R9$) after the introduction of NO_x into system, making signals of certain HOMs from other channels lower than the detection limit of the instrument. The proportions of other reaction channels decreased, and were reassigned to the NO channel, as evidenced by the fact that most of observed oxidation products were organonitrates, which is in an excellent agreement with the modeled channel proportions in Section 3.1.

Many organonitrates were observed in both series of experiments. In the low [OH] experiments, the most significant compound was $C_9H_{13}NO_8$, whose formula matches the NO termination product of $C_9H_{13}O_7^{\cdot}$, i.e., autoxidation product of BPR. The second most important compound, $C_9H_{14}N_2O_{10}$ in our low [OH] experiments, was the most significant product in the high [OH] experiments in presence of NO_x, whose formula matches the NO termination product of $C_9H_{14}NO_9^{\cdot}$, i.e., the RO_2 formed via an OH addition to $C_9H_{13}NO_6$, the NO termination product of BPR. All of the products and radicals

mentioned above were observed in Exp. 2-7, as shown in Figure 5c. From the perspective of molecular formula, $C_9H_{14}N_2O_{10}$ is also one of the most frequently observed multi-nitrogen-containing compound in polluted atmospheres, whose seasonal variations show a good correlation with [OH] (Guo et al., 2022; Yang et al., 2023).

A comparison of relative abundances of C9 and C18 products under different [OH] levels is helpful for the elucidation of their formation pathways. The difference in product distributions between Exp. 2-3 ([OH] = ~1.69×10^7 molecule cm^{-3}) and Exp. 2-1 ([OH] = ~1.03×10^8 molecule cm^{-3}), as well as between Exp. 2-3 and Exp. 1-12 ([OH] = ~8.47×10^8 molecule cm^{-3}) is shown in Figure 6. The normalized abundance was obtained by normalizing all the products to the most abundant one in each experiment, i.e., $C_{18}H_{26}O_{10}$ in Exp. 2-1 and Exp. 2-3, and $C_9H_{14}O_7$ in Exp. 1-12. The changes in the normalized abundance were obtained by subtracting the normalized abundance in Exp. 2-1 from that in Exp. 2-3, and Exp. 1-12 from Exp. 2-3. As the [OH] and OH exposure increased, there was a noticeable rise in the relative abundance of more oxygenated compounds, which can be attributed to the more intensive proportion of multi-generation OH oxidation in high OH exposure experiments. This comparison demonstrates the capacity and potential of multi-generation OH oxidation to reduce DBE and elevate the oxygenated levels of oxidation products.

In conclusion, observation of the same low DBE compounds, i.e., DBE = 2, in both low [OH] and high [OH] experiments confirms the feasibility of the generation of HOMs under atmospheric relevant conditions. The detection of $C_9H_{14}O_5$, $C_9H_{15}O_8^{\cdot}$, $C_9H_{14}O_7$, $C_9H_{14}O_8$, $C_9H_{15}O_7^{\cdot}$, and $C_9H_{16}O_8$, and $C_9H_{14}O_6$, $C_9H_{15}O_9^{\cdot}$, $C_9H_{14}O_8$, $C_9H_{14}O_9$, $C_9H_{15}O_8^{\cdot}$, and $C_9H_{16}O_9$, in low [OH] experiments also confirms the potential existence of the proposed mechanisms, i.e., Scheme 2 and Scheme 3, respectively. Certainly, other potential formation pathways for these products are possible.

”

(a)

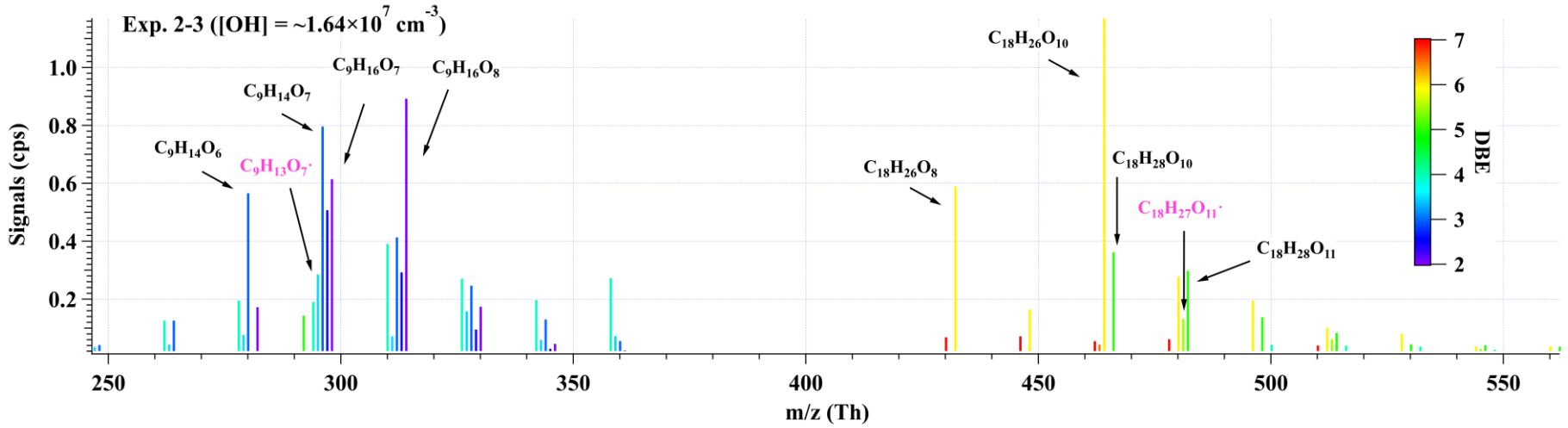
Exp. 2-3 ([OH] = ~1.64×10^7 cm^-3)
Signals (cps)
m/z (Th)
DBE
C9H14O6
C9H13O7·
C9H14O7
C9H16O7
C9H16O8
C18H26O8
C18H26O10
C18H28O10
C18H27O11·
C18H28O11

(b)

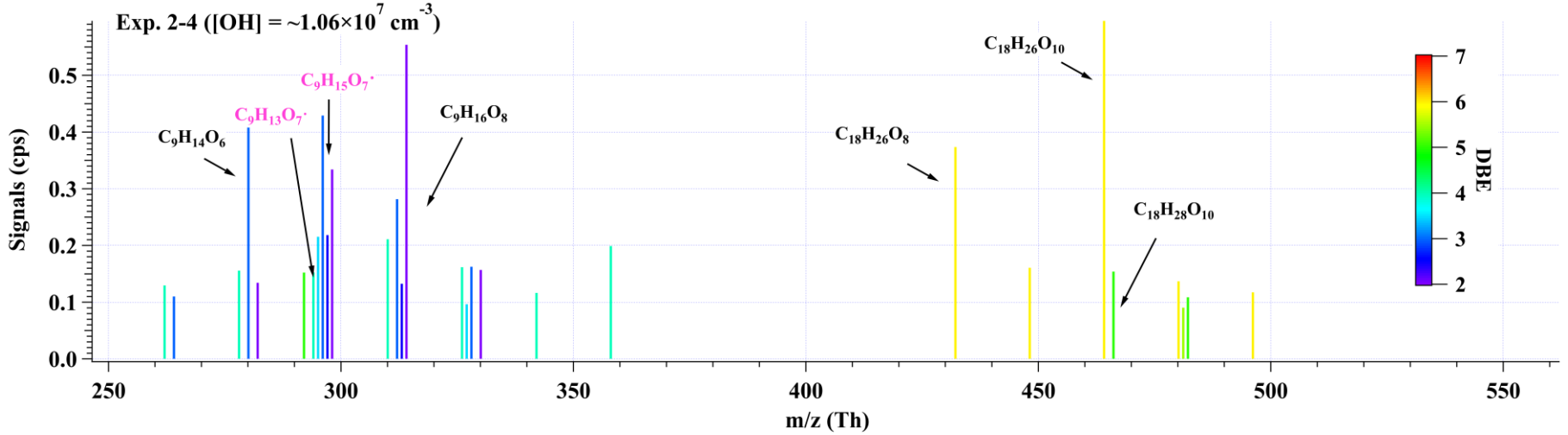
Exp. 2-4 ([OH] = ~1.06×10^7 cm^-3)
Signals (cps)
m/z (Th)
DBE
C9H14O6
C9H13O7·
C9H15O7·
C9H16O8
C18H26O8
C18H26O10
C18H28O10

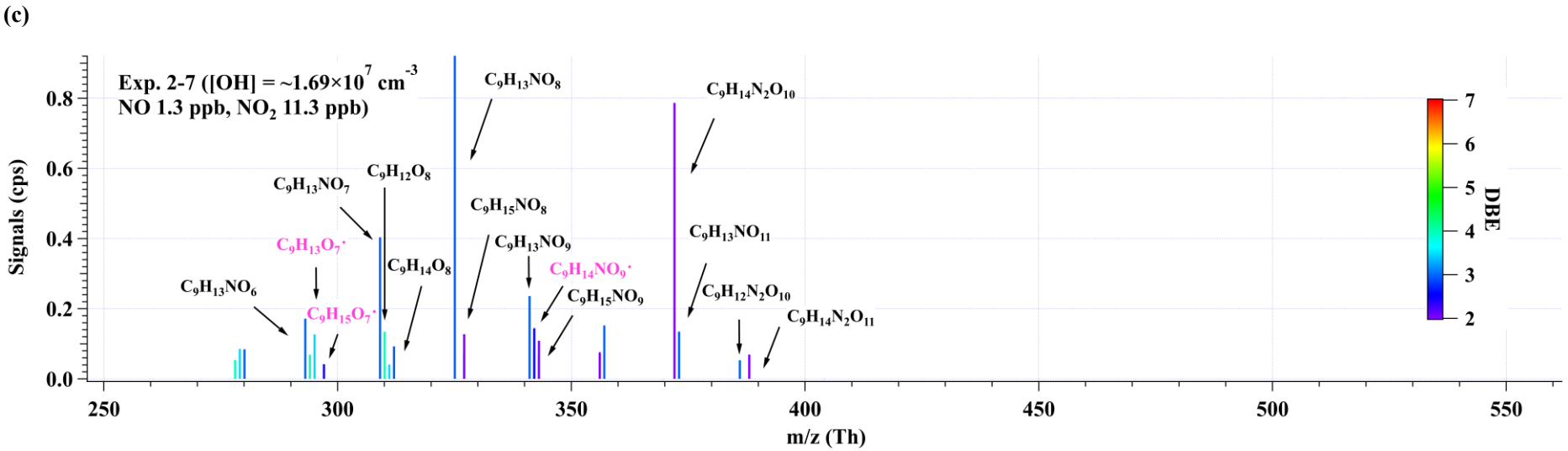

Figure 5. Distributions of C9 and C18 products detected by nitrate CI-TOF in (a) Exp. 2-3, (b) Exp. 2-4, and (c) Exp. 2-7. The reagent ion, NO_3^-, is omitted in the label for the molecular formula. Important radicals were labelled in pink. Note that no convinced signals of HOM dimers were observed in the 2nd-round experiments with NO_x.

(a)

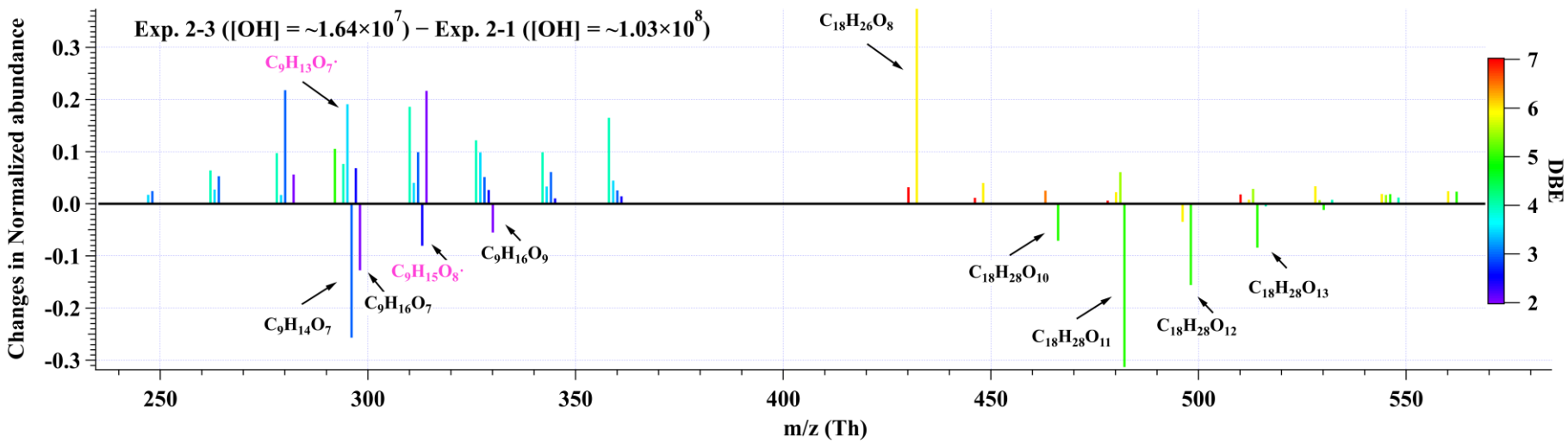
Exp. 2-3 ([OH] = ~1.64×10^7) − Exp. 2-1 ([OH] = ~1.03×10^8)
Changes in Normalized abundance
m/z (Th)
DBE
C9H13O7·
C9H15O8·
C18H26O8
C9H14O7
C9H16O7
C9H16O9
C18H28O10
C18H28O11
C18H28O12
C18H28O13

(b)

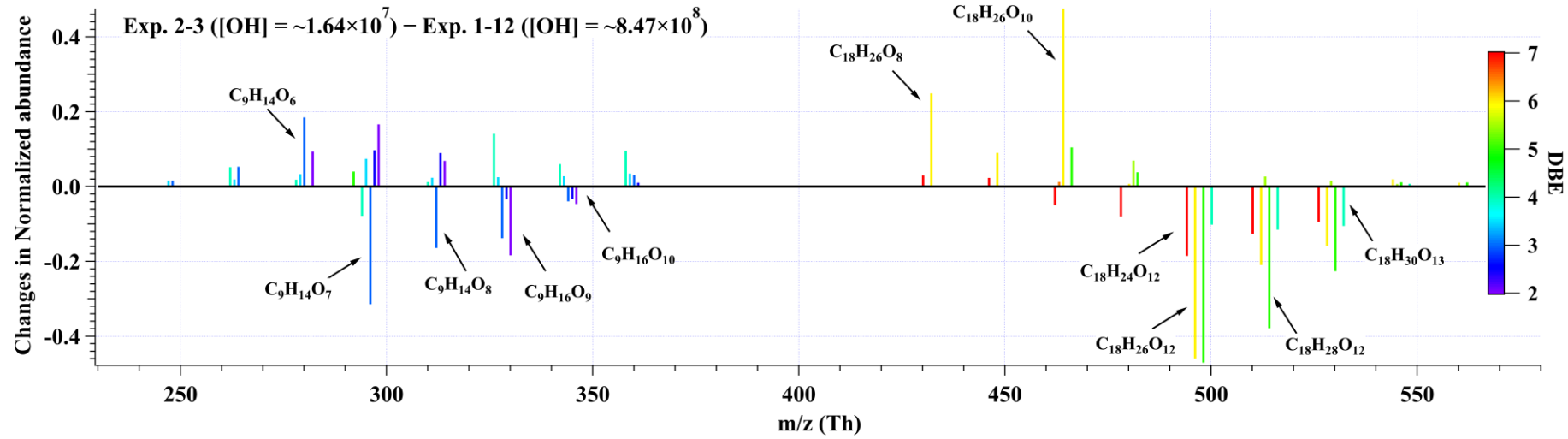
Exp. 2-3 ([OH] = ~1.64×10^7) − Exp. 1-12 ([OH] = ~8.47×10^8)
Changes in Normalized abundance
m/z (Th)
DBE
C9H14O6
C18H26O8
C18H26O10
C9H14O7
C9H14O8
C9H16O9
C9H16O10
C18H24O12
C18H26O12
C18H28O12
C18H30O13

Figure 6. The changes in normalized abundance of C9 and C18 products observed by nitrate CI-TOF in (a) Exp.2-3 relative to Exp.2-1, and (b) Exp.2-3 relative to Exp.1-12. The reagent ion, NO_3^-, is omitted in the label. The normalized abundance was obtained by normalizing all the products to the most abundant one in each experiment, i.e., $C_{18}H_{26}O_{10}$ in Exp.2-1 and Exp.2-3, and $C_9H_{14}O_7$ in Exp.1-12.

R 1.3. Updates on the results of High [OH] experiments

The estimation on the chemical fate of RO_2 in the high [OH] experiments has been updated, using the updated autoxidation reaction rate of BPR (0.078 s^{-1}). The radical concentrations estimated by the model have also been updated, due to the updates of kinetics and the input RH values. The obtained chemical fate of RO_2 in the high [OH] regime is compared with that in the low [OH] experiments, as shown in **R 1.4**.

Section 3.1 in the revised manuscript (version R2) has been updated accordingly.

R 1.4. Comparison of chemical regimes

We acknowledge that the issue with our high [OH] experiments lies in the scaling of certain pathways, i.e., all the bimolecular reactions, to unrealistic levels, thereby facilitating observation of reaction products that are in fact minor in the ambient.

In our previous reply, the analysis on chemical regimes and the fate of RO_2 is intended to clarify that the decrease of DBE of products comes from the addition of OH to the stabilized products, and the hydroxyl termination reaction ($R3$) or hydroperoxyl termination reaction ($R5$) of RO_2. Though reaction $R6$ between OH and RO_2 can potentially generate ROOOH that is also a possible pathway to decrease DBE, its contribution is quite limited due to its low yield. Also, under our high [OH] experiments, [HO_2] and [RO_2] both increased with [OH], while the ratios of HO_2:OH:RO_2 were generally not far from those under ambient conditions. Hence, the ratios for monomeric termination products generated by those monomeric termination reactions, i.e., $R1$ - $R3$ and $R5$ - $R6$, are atmospheric relevant, which are able to alter the DBE of products without influencing their carbon chains.

The radical concentrations were estimated by the PAM_chem_v8 model to illustrate the chemical regimes in the 2nd-round experiments (Table R2). The average [HO_2], [OH], and [RO_2] were 9.7×10^7, 1.64×10^7, and 1.69×10^9 molecule cm^{-3}, respectively, in Exp. 2-3, and were 6.7×10^7, 1.04×10^7, and 1.34×10^9 molecule cm^{-3}, respectively, in Exp. 2-4, both of which generally differ by no more than a factor of 3 from the summer daytime ambient ones in polluted atmospheres (Tan et al., 2017, 2018, 2019; Whalley et al., 2021; Lu et al., 2012). The average [HO_2], [OH], and [RO_2], as well as the NO and NO_2 concentrations in Exp. 2-7 are generally very close to those in the same environment (Tan et al., 2019).

Table R2. Summary of radical concentrations estimated by the PAM_chem_v8 model in the 2nd-round experiments.

	Estimated [OH] with PAM_chem_v8 based on the precursor consumption ($\times10^7$ molecule cm^{-3})	Estimated [HO_2] with PAM_chem_v8 based on the precursor consumption ($\times10^8$ molecule cm^{-3})	Estimated [RO_2] with PAM_chem_v8 based on the precursor consumption ($\times10^9$ molecule cm^{-3})
2-1	10.3	3.73	4.05
2-2	4.54	2.14	2.80
2-3	1.64	0.97	1.69
2-4	1.04	0.67	1.34
2-5	5.80	13.1	1.55
2-6	3.69	11.5	1.39
2-7	1.69	8.38	1.07

To make the discussion clearer, in this reply we follow the sequential labels of different reactions of

RO_2 as below:

$$RO_2 + R'O_2 \rightarrow RO + R'O + O_2 \quad (R1)$$
$$RO_2 + R'O_2 \rightarrow R=O + R'OH + O_2 \quad (R2)$$
$$RO_2 + R'O_2 \rightarrow ROH + R'=O + O_2 \quad (R3)$$
$$RO_2 + R'O_2 \rightarrow ROOR' + O_2 \quad (R4)$$
$$RO_2 + HO_2 \rightarrow ROOH + O_2 \quad (R5)$$
$$RO_2 + OH \rightarrow Products \quad (R6)$$
$$RO_2 \xrightarrow{isomerization} Products \quad (R7)$$
$$RO_2 + NO \rightarrow RO + NO_2 \quad (R8)$$
$$RO_2 + NO \rightarrow RONO_2 \quad (R9)$$
$$RO_2 \rightarrow physical\ loss \quad (R10)$$

We take Exp. 1-12 ([OH] = ~8.47×10^8 molecule cm^{-3} and NO_x = 0) and Exp. 2-3 ([OH] = ~1.64×10^7 molecule cm^{-3} and NO_x = 0) as representative examples and compare simulation results with those from the ambient atmosphere, since NO_x in the ambient is believed not to impact relative ratios for R1-R3, R5, and R6. In the ambient atmosphere, the average [HO_2], [OH], and [RO_2] were 2.7×10^8, 8.0×10^6, and 1.4×10^9 molecule cm^{-3}, respectively, around summertime noon in urban Beijing (Whalley et al. 2021), and (4 - 28)$\times10^8$, (0.8 - 2.4)$\times10^7$, and 1.2×10^9 molecule cm^{-3} (modeled) at a suburban site in Yangtze River Delta (Ma et al. 2022). As shown in Figure R3a (also as Figure 1a in the revised manuscript, version R2), for the most important RO_2, BPR, the fractions of monomeric termination reactions of RO_2 + RO_2 ($R1 - R3$), RO_2 + HO_2 ($R5$), and RO_2 + OH ($R6$) were 6.2%, 29.3%, and 64.5%, respectively, in Exp. 1-12. In contrast, the fractions were 32.5%, 31.8%, and 35.7%, respectively, in Exp. 2-3, whereas the values were 20.3%, 66.6%, and 13.2%, respectively, for summertime, urban Beijing.

Our NO_x-free experiments are characterized with an inherent drawback that the proportion of the HO_2 termination pathway ($R5$) is actually lower than that under ambient conditions, which is similar to most other laboratory experiments (Bianchi et al., 2019). In our high [OH] experiments without NO_x, the reaction rates of unimolecular reactions e.g., autoxidation reaction ($R7$) and condensation ($R10$) did not change with [OH] that increased in our experiments relative to that in the ambient. As a result, relative proportions of autoxidation and condensation are lowered. On the other hand, 1,3,5-TMB-derived BPR was suggested to undergo autoxidation ($R7$) at a reaction rate of 0.078 s^{-1} (Wang et al., 2017), which represents 36.8%, 94.4%, and 92.8% of the overall rates of $R1$ - $R3$ and $R5$ - $R7$ in Exp. 1-12, Exp. 2-3, and summertime, urban Beijing, respectively. Because of its dominant proportion in Exp. 2-3 and the ambient, the autoxidation channel is not included for clarity in Figure R3a. Autoxidation does possess a lower significance in our high [OH] experiments due to the other accelerated bimolecular reactions. However, it would only influence the oxygen content of our products but would not change the DBE. Both accretion reaction ($R4$) and condensation ($R10$) have been taken into account in the model, but they would not influence the distributions of monomeric stabilized products. We will specifically discuss these two pathways in the following sections because of their complexity between the laboratory and ambient conditions.

RO_2 other than BPR and $C_9H_{13}O_7$· existed in the PAM OFR, which were not included in the model simulation. Their reaction rates of the accretion reaction ($R4$) and the autoxidation reaction ($R7$) should be different from BPR and $C_9H_{13}O_7$· due to the strong dependence of these two reaction rates on the molecular structure. Rates for the other channels, on the other hand, should be the same as those of BPR and $C_9H_{13}O_7$·. Therefore, their fates in terms of the monomeric termination reactions ($R1$ - $R3$, $R5$ - $R6$, and $R8$ - $R9$)

should be similar as BPR and $C_9H_{13}O_7^{\cdot}$.

Calculated from yields of stabilized monomeric termination products of BPR, the fractions of monomeric termination reaction products in Exp. 1-12, Exp. 2-3, and summertime, urban Beijing (Whalley et al. 2021) are presented in Figure R3b (also as Figure 1b in the revised manuscript, version R2), showing a lot of similarities between these conditions. The fractions of R=O, ROH, ROOH, and ROOOH in Exp. 1-12 were 3.1%, 14.1%, 71.7%, and 11.1%, respectively. These fractions were 13.0%, 18.1%, 63.9%, and 5.0%, respectively, in the Exp. 2-3, whereas the values were 5.3%, 6.5%, 87.0%, and 1.2%, respectively, in the summertime Beijing case. Among them, the majority of products are always ROOH and ROH, with ROOH being the most abundant. Therefore, the monomeric termination products of BPR in our experiments are atmospheric relevant. In addition, only the R=O product has a DBE higher than the reacted RO_2, but merely accounted for a limited proportion. All the other stabilized termination products have a DBE that is 1 lower than the precursor, and are the majority in both laboratory and ambient conditions. This indicates that the majority of the first-generation products typically have a DBE that is 1 lower than that of 1,3,5-TMB, whereas the majority of subsequent-generation products typically have a DBE that is 2 lower than that of 1,3,5-TMB. Once a monomeric compound with a DBE that is ≥2 lower than that of 1,3,5-TMB was observed, multi-generation OH reactions have happened in the system.

In experiments in absence of NO_x (e.g., Exp.1-12), the proportions of $R8$ - $R9$, i.e., the NO channel in the urban atmosphere were attributed to termination reactions of $R1$ - $R6$, i.e., $RO_2 + RO_2$, accretion reaction, $RO_2 + HO_2$, and $RO_2 + OH$. By expanding proportions of these termination reactions, laboratory investigations on product distributions can be facilitated, as the detection of certain HOM products became more precise and the mass spectra became simplified.

(a)

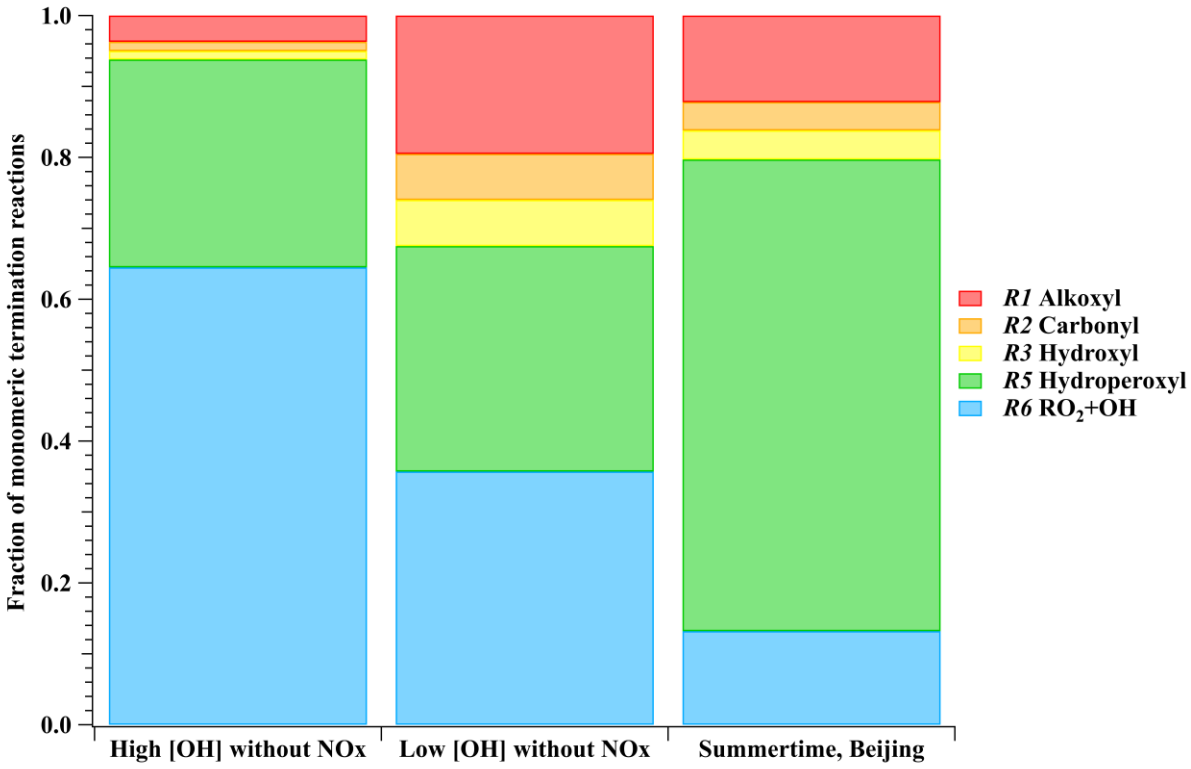

(b)

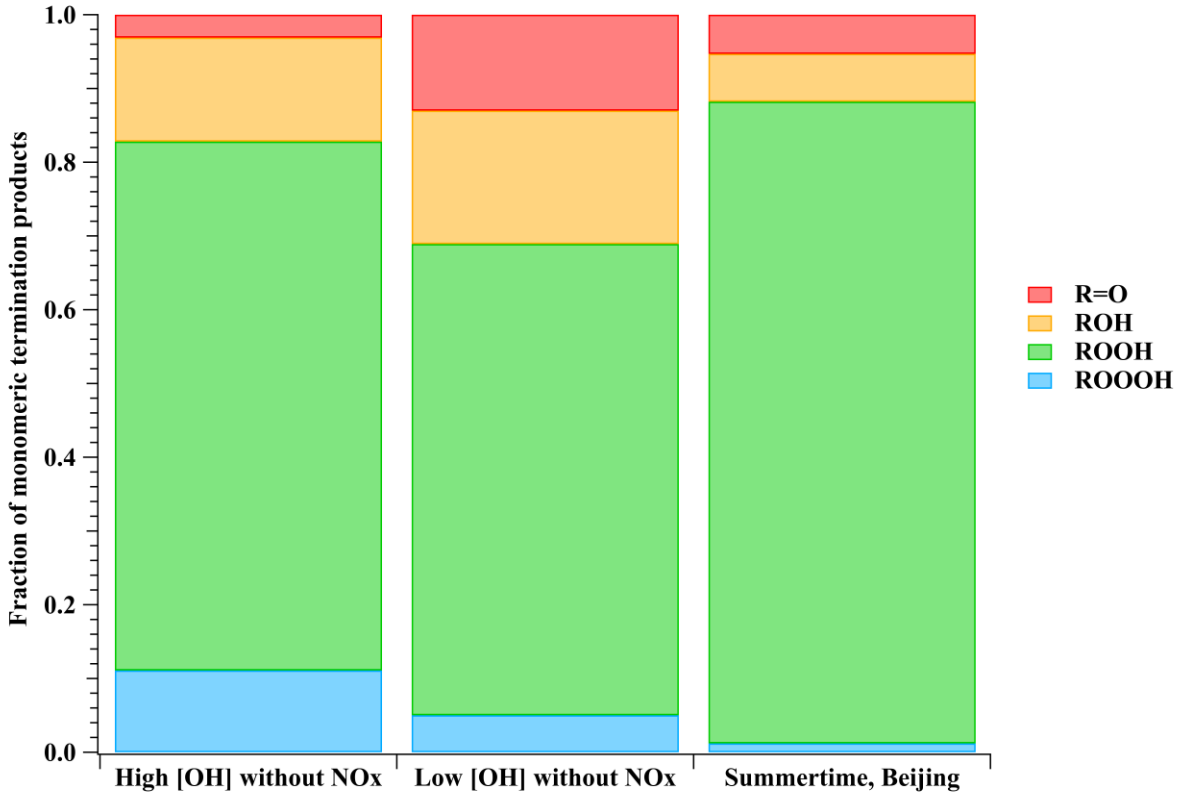
Fraction of monomeric termination products
1.0
0.8
0.6
0.4
0.2
0.0
High [OH] without NOx
Low [OH] without NOx
Summertime, Beijing
R=O
ROH
ROOH
ROOOH

(c)

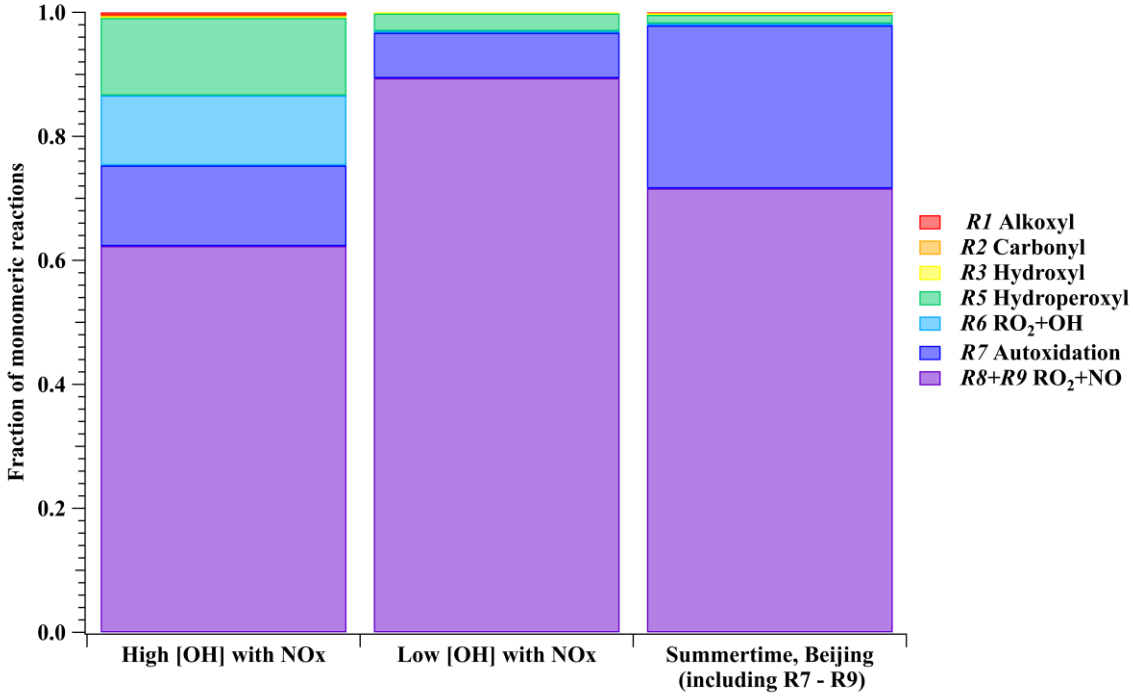
Fraction of monomeric reactions
1.0
0.8
0.6
0.4
0.2
0.0
High [OH] with NOx
Low [OH] with NOx
Summertime, Beijing
(including R7 - R9)
R1 Alkoxyl
R2 Carbonyl
R3 Hydroxyl
R5 Hydroperoxyl
R6 RO2+OH
R7 Autoxidation
R8+R9 RO2+NO

(d)

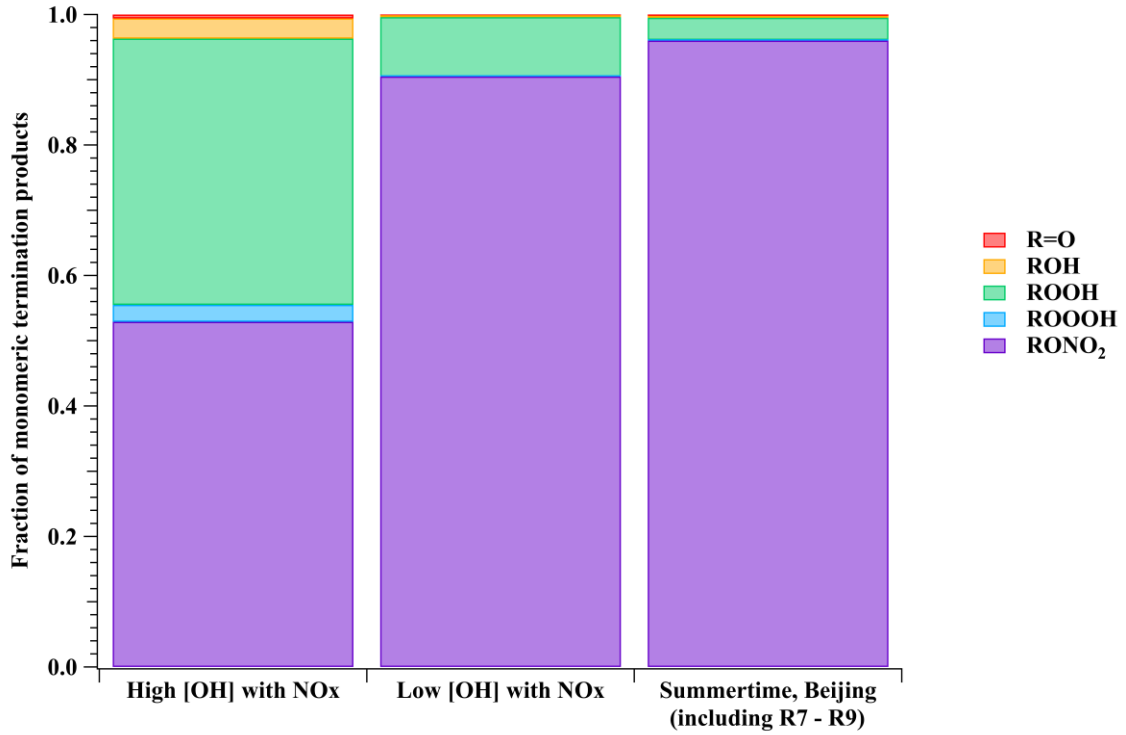

Figure R3. (a) The fraction of monomeric termination reactions and (b) monomeric termination products of BPR in a representative high [OH] experiment without NO_x (Exp. 1-12), a representative low [OH] experiment without NO_x (Exp. 2-3), and summertime, urban Beijing (Whalley et al. 2021). NO_x related reactions and products for the Beijing study are not included for a better comparison. (c) The fraction of monomeric reactions (R1 - R3 and R5 - R9) and (d) monomeric termination products of BPR in a representative high [OH] experiment with NO_x (Exp. 1-48), a representative low [OH] experiment with NO_x (Exp. 2-7), and summertime, urban Beijing (Whalley et al. 2021). Reactions and kinetic rate coefficients used in the calculations are provided in Table S2.

In experiments with NO_x, the chemical fates of BPR in high [OH] experiments (Exp. 1-48 as an example, [OH] = ~6.77×10^8 molecule cm^{-3}, NO = ~1.93 ppb. NO_2 = ~68 ppb), low [OH] experiments (Exp. 2-7 as an example, [OH] = ~1.69×10^7 molecule cm^{-3}, NO = ~1.30 ppb. NO_2 = ~11 ppb), and the summertime, urban Beijing are compared. As shown in Figure R3c (also as Figure 1c in the revised manuscript, version R2), in all three conditions, RO_2 reactions with NO were always the most significant pathway, with autoxidation being the second most significant.

Accounting for at least 52% of monomeric termination products under all conditions, organonitrates were always the most important termination products, as shown in Figure R3d (also as Figure 1d in the revised manuscript, version R2). On the other hand, based on the formulae of organonitrates, the detailed formulae for monomer RO_2 could be probed, which can help us better understand the chemical reactions inside the system.

Due to the complexity of ambient RO_2 pool, it is difficult to estimate the detailed fraction of accretion reactions *R*4. In the laboratory experiments, RO_2 pool mainly consists of BPR and its autoxidation reaction product $C_9H_{13}O_7\cdot$, which both can undergo accretion reaction rapidly (Berndt et al., 2018). The concentrations of these two radicals were estimated by PAM_chem_v8 according to the kinetics discussed in Section S1. The reaction rate of accretion reaction (*R*4) for BPR was around 1.61 s^{-1} in Exp. 1-12, being

61.8% of $R1-R7$, and was 0.29 s^{-1} in Exp. 2-3, equivalent to 21.1% of $R1-R7$. Certain uncertainties exist in the estimation of the proportions of accretion reactions, as the PAM_chem_v8 model only includes the first-generation reactions of precursors, whereas the subsequential fragmentation and re-initiation of stabilized products can generate a series of new RO_2 that will influence the proportions of accretion reactions. We are only certain that the significance of accretion reactions in both Exp. 1-12 and Exp. 2-3 is larger than the ambient. However, this deviation will not influence our conclusion on multi-generation OH oxidation. Nevertheless, the dimer products generally help us identify the exact RO_2 in the OFR, and confirm the conditions of secondary OH oxidation according to the number of hydrogen atoms in the molecules, as we have already pointed out in Section 3.1 of the last manuscript (version R1).

In addition, certain compounds might have condensed onto pre-existing particles in the real atmosphere before an appreciable fraction of such compounds undergoes the re-initiated OH oxidation. Therefore, even the same product can be generated both in the laboratory experiments and the ambient atmosphere, the relative significance of this product is not completely identical. Though OOMs might have the potential to undergo multi-generation OH oxidation, the exact proportion of this reaction in the ambient strongly depends on their volatility, in other words, condensation sink of these OOMs. The typical monomeric termination products of 1,3,5-TMB-derived BPR, $C_9H_{12}O_4$, $C_9H_{14}O_4$, $C_9H_{14}O_5$, and $C_9H_{13}NO_6$, are estimated to have saturation vapor concentrations (C*) of 30.20, 30.20, 0.85, and 3.39 μg/m^3 at 300 K with the volatility parameterization developed in the CLOUD chamber oxidation experiments of aromatics, respectively (Wang et al., 2020a). From the perspective of volatility, they all belong to semi-volatile organic compounds (SVOC, 0.3 < C* < 300 μg/m^3) and are expected to exist in both the condensed and the gas phases at equilibrium in the atmosphere (Bianchi et al., 2019). Compared to ambient conditions, their condensation rates in the laboratory were biased to be lower due to the accelerated bimolecular reactions. However, this will not prevent the high [OH] experiments from showing the potential and ability of these compounds to go through re-initiated OH oxidation, as these compounds would exist in significant fractions in the gas phase in the real atmosphere.

However, the conditions are completely distinct for other HOM monomer products and HOM dimer products with much lower volatility. It is difficult for a HOM dimer, e.g., $C_{18}H_{26}O_{10}$ estimated with a C* of 7.24×10^{-13} μg/m^3 at 300 K, to survive long enough to experience an appreciable re-initiated photochemical ageing. The lifetime of HOMs that can be classified as low volatile organic compounds (LVOCs, 3×10^{-5} < C* < 0.3 μg/m^3) and extremely low volatile organic compounds (ELVOCs, C* < 3×10^{-5} μg/m^3) can be estimated according to the condensation sink (CS) in the atmosphere, as they are lost irreversibly onto surfaces. The median value of CS in urban Beijing was reported to be around 0.019 s^{-1} and 0.057 s^{-1} during NPF days and non-NPF days, respectively, whereas the values in Shanghai were reported to be around 0.013 s^{-1} and 0.017 s^{-1}. respectively (Deng et al., 2020; Yao et al., 2018), which are all much higher than the physical loss in our PAM OFR, i.e., 0.0023 s^{-1}, as stated in Section S1. LVOCs and ELVOCs are believed to be lost irreversibly to the surface in both the laboratory and the ambient because of their low volatility. However, by assuming a similar diffusion coefficient of LVOCs and ELVOCs to that of sulfuric acid, the lifetimes of LVOCs and ELVOCs in the ambient can be estimated to be as high as 77 s for the condensation loss, which is close to the residence time of our PAM OFR. Therefore, LVOCs and ELVOCs should at least have the potential to experience the same OH exposures in the ambient as those in our low [OH] experiments, i.e., at least 5.86×10^8 molecule cm^{-3} s, if they were generated. On the other hand, the detailed proportions of LVOCs and ELVOCs after a large OH exposure should be lower than those in the lab due to their magnified physical loss in the ambient. This means that if the multi-generation products of those compounds were observed in the ambient air, they should have been generated via a reaction that happened very recently.

This part corresponds to **Section 3.1** in the revised manuscript (version R2).

We have revised our manuscript (Line 328 - 539) as:

"**3.1 Comparison of chemical regimes**

Concentration profiles of OH, RO_2, and HO_2 as a function of OH exposures in our high [OH] experiments without NO_x, i.e., the 1st-round experiments, are illustrated in Figure S1a. According to the modified PAM_chem_v8, when [OH] increased from 9.32×10^7 to 1.03×10^9 molecule cm^{-3}, [HO_2] increased from 7.25×10^8 to 2.79×10^9 molecule cm^{-3}, whereas [RO_2] concentrations increased from 5.17×10^9 to 9.5×10^9 molecule cm^{-3}. The radical concentrations in high [OH] experiments with NO_x (Figure S1b) varied in a similar range, with [RO_2] ranging from 4.38×10^9 to 9.13×10^9 molecule cm^{-3}, HO_2 ranging from 4.47×10^9 to 6.47×10^9 molecule cm^{-3}, and OH ranging from 3.86×10^8 to 7.82×10^8 molecule cm^{-3}, respectively. The ratios between HO_2/OH and RO_2/OH in the 1st-round experiments were generally in the same order of magnitude with the ambient atmosphere (Whalley et al., 2021).

Radical concentrations were also estimated by the PAM_chem_v8 model to illustrate the chemical regimes in the 2nd-round experiments (Table S4). The average [HO_2], [OH], and [RO_2] were 9.7×10^7, 1.64×10^7, and 1.69×10^9 molecule cm^{-3}, respectively, in Exp. 2-3, and were 6.7×10^7, 1.04×10^7, and 1.34×10^9 molecule cm^{-3}, respectively, in Exp. 2-4, both of which generally differ by no more than a factor of 3 from the summer daytime ambient ones in polluted atmosphere (Tan et al., 2017, 2018, 2019; Whalley et al., 2021; Lu et al., 2012). The average [HO_2], [OH], and [RO_2], as well as the NO and NO_2 concentrations in Exp. 2-7 are generally very close to those in the same environment (Tan et al., 2019).

(a)

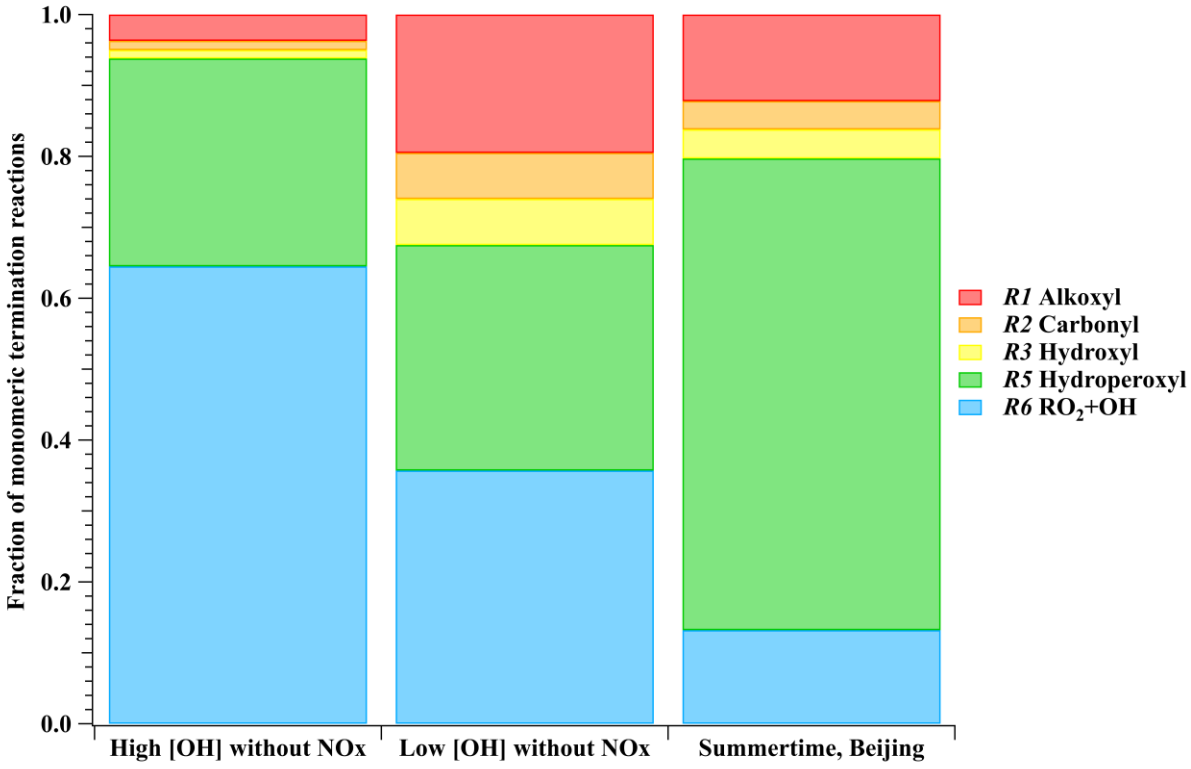

(b)

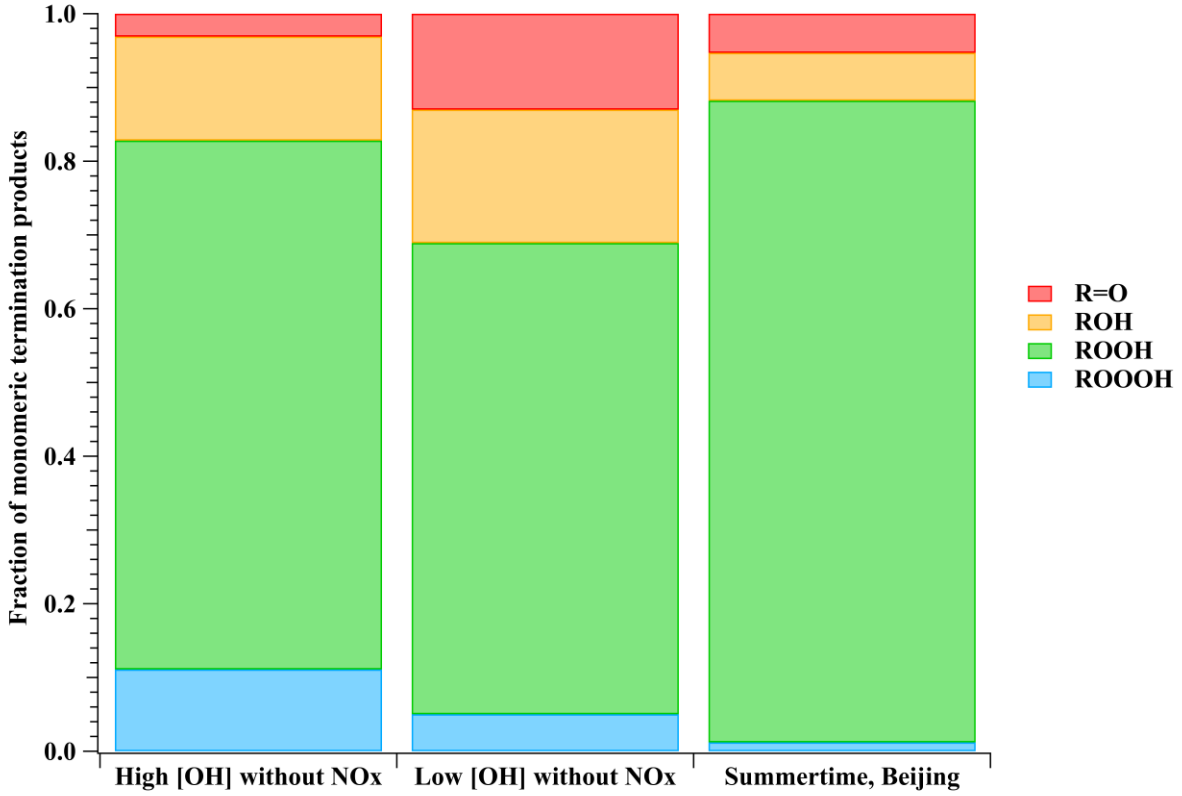
Fraction of monomeric termination products
1.0
0.8
0.6
0.4
0.2
0.0
High [OH] without NOx
Low [OH] without NOx
Summertime, Beijing
R=O
ROH
ROOH
ROOOH

(c)

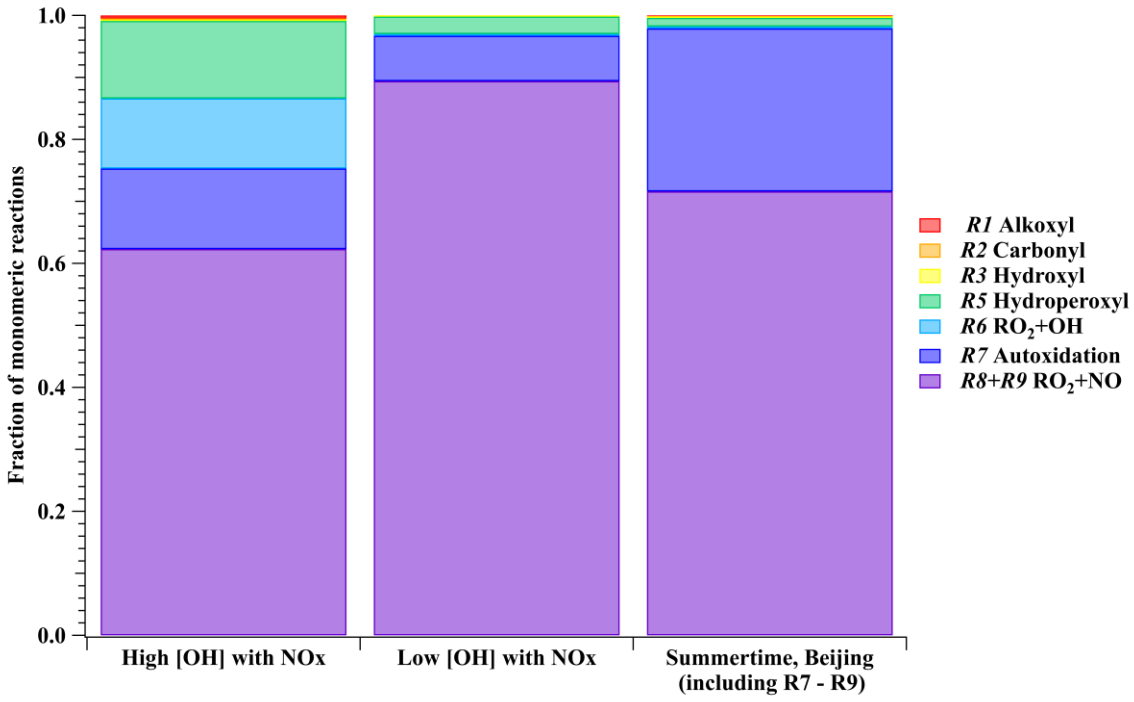
Fraction of monomeric reactions
1.0
0.8
0.6
0.4
0.2
0.0
High [OH] with NOx
Low [OH] with NOx
Summertime, Beijing
(including R7 - R9)
R1 Alkoxyl
R2 Carbonyl
R3 Hydroxyl
R5 Hydroperoxyl
R6 RO2+OH
R7 Autoxidation
R8+R9 RO2+NO

(d)

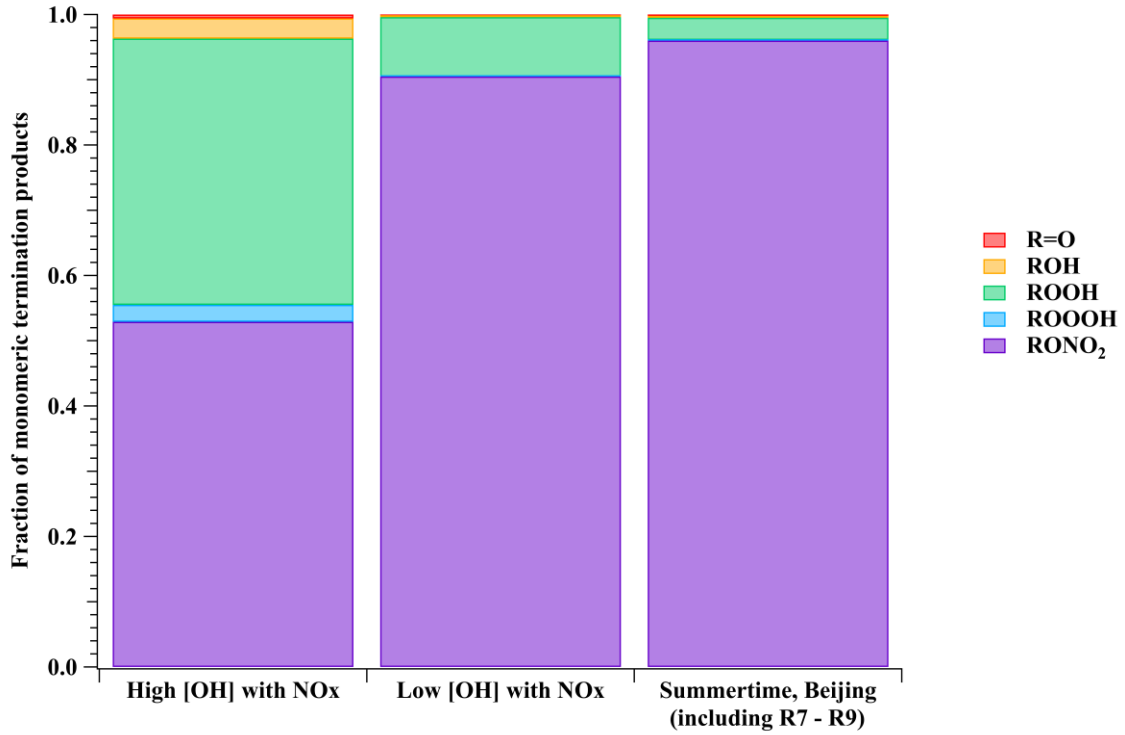

Figure 1. (a) The fraction of monomeric termination reactions and (b) monomeric termination products of BPR in a representative high [OH] experiment without NO_x (Exp. 1-12), a representative low [OH] experiment without NO_x (Exp. 2-3), and summertime, urban Beijing (Whalley et al. 2021). NO_x related reactions and products for the Beijing study are not included for a better comparison. (c) The fraction of monomeric reactions (R1 - R3 and R5 - R9) and (d) monomeric termination products of BPR in a representative high [OH] experiment with NO_x (Exp. 1-48), a representative low [OH] experiment with NO_x (Exp. 2-7), and summertime, urban Beijing (Whalley et al. 2021). Reactions and kinetic rate coefficients used in the calculations are provided in Table S2.

We take Exp. 1-12 ([OH] = ~8.47×10^8 molecule cm^{-3} and NO_x = 0) and Exp. 2-3 ([OH] = ~1.64×10^7 molecule cm^{-3} and NO_x = 0) as representative examples and compare simulation results with those from the ambient atmosphere, since NO_x in the ambient is believed not to impact relative ratios for $R1 - R3$, $R5$, and $R6$. In the ambient atmosphere, the average [HO_2], [OH], and [RO_2] were 2.7×10^8, 8.0×10^6, and 1.4×10^9 molecule cm^{-3}, respectively, around summertime noon in urban Beijing (Whalley et al. 2021), and (4 - 28)$\times10^8$, (0.8 - 2.4)$\times10^7$, and 1.2×10^9 molecule cm^{-3} (modeled) at a suburban site in Yangtze River Delta (Ma et al. 2022). As shown in Figure 1a, for the most important RO_2, BPR, the fractions of monomeric termination reactions of RO_2 + RO_2 ($R1 - R3$), RO_2 + HO_2 ($R5$), and RO_2 + OH ($R6$) were 6.2%, 29.3%, and 64.5%, respectively, in Exp.1-12. In contrast, the fractions were 32.5%, 31.8%, and 35.7%, respectively, in Exp. 2-3, whereas the values were 20.3%, 66.6%, and 13.2%, respectively, for summertime, urban Beijing.

Our NO_x-free experiments are characterized with an inherent drawback that the proportion of the HO_2 termination pathway ($R5$) is actually lower than that under ambient conditions, which is similar to most other laboratory experiments (Bianchi et al., 2019). In our high [OH] experiments without NO_x, the reaction rates of unimolecular reactions e.g., autoxidation reaction ($R7$) and condensation ($R10$) did not change with [OH] that increased in our experiments relative to that in the ambient. As a result, relative proportions of autoxidation and condensation are lowered. On the other hand, 1,3,5-TMB-derived BPR was suggested to

undergo autoxidation ($R7$) at a reaction rate of 0.078 s^{-1} (Wang et al., 2017), which represents 36.8%, 94.4%, and 92.8% of the overall rates of $R1$ - $R3$ and $R5$ - $R7$ in Exp. 1-12, Exp. 2-3, and summertime, urban Beijing, respectively. Because of its dominant proportion in Exp. 2-3 and the ambient, the autoxidation channel is not included for clarity in Figure 1a. Autoxidation does possess a lower significance in our high [OH] experiments due to the other accelerated bimolecular reactions. However, it would only influence the oxygen content of our products but would not change the DBE. Both accretion reaction ($R4$) and condensation ($R10$) have been taken into account in the model, but they would not influence the distributions of monomeric stabilized products. We will specifically discuss these two pathways in the following sections because of their complexity between the laboratory and ambient conditions.

RO_2 other than BPR and $C_9H_{13}O_7$· existed in the PAM OFR, which were not included in the model simulation. Their reaction rates of the accretion reaction ($R4$) and the autoxidation reaction ($R7$) should be different from BPR and $C_9H_{13}O_7$· due to the strong dependence of these two reaction rates on the molecular structure. Rates for the other channels, on the other hand, should be the same as those of BPR and $C_9H_{13}O_7$·. Therefore, their fates in terms of the monomeric termination reactions ($R1$ - $R3$, $R5$ - $R6$, and $R8$ - $R9$) should be similar as BPR and $C_9H_{13}O_7$·.

Calculated from yields of stabilized monomeric termination products of BPR, the fractions of monomeric termination reaction products in Exp. 1-12, Exp. 2-3, and summertime, urban Beijing (Whalley et al. 2021) are presented in Figure 1b, showing a lot of similarities between these conditions. The fractions of R=O, ROH, ROOH, and ROOOH in Exp. 1-12 were 3.1%, 14.1%, 71.7%, and 11.1%, respectively. These fractions were 13.0%, 18.1%, 63.9%, and 5.0%, respectively, in the Exp. 2-3, whereas the values were 5.3%, 6.5%, 87.0%, and 1.2%, respectively, in the summertime Beijing case. Among them, the majority of products are always ROOH and ROH, with ROOH being the most abundant. Therefore, the monomeric termination products of BPR in our experiments are atmospheric relevant. In addition, only the R=O product has a DBE higher than the reacted RO_2, but merely accounted for a limited proportion. All the other stabilized termination products have a DBE that is 1 lower than the precursor, and are the majority in both laboratory and ambient conditions. This indicates that the majority of the first-generation products typically have a DBE that is 1 lower than that of 1,3,5-TMB, whereas the majority of subsequent-generation products typically have a DBE that is 2 lower than that of 1,3,5-TMB. Once a monomeric compound with a DBE that is ≥2 lower than that of 1,3,5-TMB was observed, multi-generation OH reactions have happened in the system.

In experiments in absence of NO_x (e.g., Exp.1-12), the proportions of $R8$ - $R9$, i.e., the NO channel in the urban atmosphere were attributed to termination reactions of $R1$ - $R6$, i.e., RO_2 + RO_2, accretion reaction, RO_2 + HO_2, and RO_2 + OH. By expanding proportions of these termination reactions, laboratory investigations on product distributions can be facilitated, as the detection of certain HOM products became more precise and the mass spectra became simplified.

In experiments with NO_x, the chemical fates of BPR in high [OH] experiments (Exp. 1-48 as an example, [OH] = ~6.77×10^8 molecule cm^{-3}, NO = ~1.93 ppb. NO_2 = ~68 ppb), low [OH] experiments (Exp. 2-7 as an example, [OH] = ~1.69×10^7 molecule cm^{-3}, NO = ~1.30 ppb. NO_2 = ~11 ppb), and the summertime, urban Beijing are compared. As shown in Figure 1c, in all three conditions, RO_2 reactions with NO were always the most significant pathway, with autoxidation being the second most significant.

Accounting for at least 52% of monomeric termination products under all conditions, organonitrates were always the most important termination products, as shown in Figure 1d. On the other hand, based on the formulae of organonitrates, the detailed formulae for monomer RO_2 could be probed, which can help us better understand the chemical reactions inside the system. Alkoxy radicals generated in the NO termination channel will unlikely influence the distributions of C9 stabilized products since they tend to get decomposed

in the subsequent reactions, as discussed in the Supplementary Text S1.

Due to the complexity of ambient RO_2 pool, it is difficult to estimate the detailed fraction of accretion reactions $R4$. In the laboratory experiments, RO_2 pool mainly consists of BPR and its autoxidation reaction product $C_9H_{13}O_7\cdot$, which both can undergo accretion reaction rapidly (Berndt et al., 2018b). The concentrations of these two radicals were estimated by PAM_chem_v8 according to the kinetics discussed in Supplementary Text S1. The reaction rate of accretion ($R4$) for BPR was around 1.61 s^{-1} in Exp.1-12, being 61.8% of $R1-R7$, and was 0.29 s^{-1} in Exp.2-3, equivalent to 21.1% of $R1-R7$. Certain uncertainties exist in the estimation of the proportions of accretion reactions, as the PAM_chem_v8 model only includes the first-generation reactions of precursors, whereas the subsequential fragmentation and re-initiation of stabilized products can generate a series of new RO_2 that will influence the proportions of accretion reactions. We are only certain that the significance of accretion reactions in both Exp. 1-12 and Exp. 2-3 is larger than the ambient. The much-expanded proportion of HOM dimers through accretion reactions makes it inadequate to compare yields of HOM dimers and HOM monomers. However, this deviation will not influence our conclusion on multi-generation OH oxidation and identification of HOM dimers can help us identify the exact RO_2 in the OFR and confirm the conditions of secondary OH oxidation according to the number of hydrogen atoms in the molecules.

In addition, certain compounds might have condensed onto pre-existing particles in the real atmosphere before an appreciable fraction of such compounds undergoes the re-initiated OH oxidation. Therefore, even the same product can be generated both in the laboratory experiments and the ambient atmosphere, the relative significance of this product is not completely identical. Though OOMs might have the potential to undergo multi-generation OH oxidation, the exact proportion of this reaction in the ambient strongly depends on their volatility, in other words, condensation sink of these OOMs. The typical monomeric termination products of 1,3,5-TMB-derived BPR, $C_9H_{12}O_4$, $C_9H_{14}O_4$, $C_9H_{14}O_5$, and $C_9H_{13}NO_6$, are estimated to have saturation vapor concentrations (C*) of 30.20, 30.20, 0.85, and 3.39 μg/m^3 at 300 K with the volatility parameterization developed in the CLOUD chamber oxidation experiments of aromatics, respectively (Wang et al., 2020a). From the perspective of volatility, they all belong to semi-volatile organic compounds (SVOC, $0.3 < C^* < 300$ μg/m^3) and are expected to exist in both the condensed and the gas phases at equilibrium in the atmosphere (Bianchi et al., 2019). Compared to ambient conditions, their condensation rates in the laboratory were biased to be lower due to the accelerated bimolecular reactions. However, this will not prevent the high [OH] experiments from showing the potential and ability of these compounds to go through re-initiated OH oxidation, as these compounds would exist in significant fractions in the gas phase in the real atmosphere.

However, the conditions are completely distinct for other HOM monomer products and HOM dimer products with much lower volatility. It is difficult for a HOM dimer, e.g., $C_{18}H_{26}O_{10}$ estimated with a C* of 7.24×10^{-13} μg/m^3 at 300 K, to survive long enough to experience an appreciable re-initiated photochemical ageing. The lifetime of HOMs that can be classified as LVOCs ($3\times10^{-5} < C^* < 0.3$ μg/m^3) and ELVOCs ($C^* < 3\times10^{-5}$ μg/m^3) can be estimated according to the condensation sink (CS) in the atmosphere, as they are lost irreversibly onto surfaces. The median value of CS in urban Beijing was reported to be around 0.019 s^{-1} and 0.057 s^{-1} during NPF days and non-NPF days, respectively, whereas the values in Shanghai were reported to be around 0.013 s^{-1} and 0.017 s^{-1}. respectively (Deng et al., 2020; Yao et al., 2018), which are all much higher than the physical loss in our PAM OFR, i.e., 0.0023 s^{-1}, as stated in the Supplementary Text S1. LVOCs and ELVOCs are believed to be lost irreversibly to the surface in both the laboratory and ambient because of their low volatility. However, by assuming a similar diffusion coefficient of LVOCs and ELVOCs to that of sulfuric acid, the lifetimes of LVOCs and ELVOCs in the ambient still can be as high as 77 s for the

condensation loss, which is close to the residence time of our PAM OFR. Therefore, LVOCs and ELVOCs should at least have the potential to experience the same OH exposures in the ambient as those in our low [OH] experiments, i.e., at least 5.86×10^{8} molecule cm^{-3} s, if they were generated. On the other hand, the detailed proportions of LVOCs and ELVOCs after a large OH exposure should be lower than those in the lab due to their magnified physical loss in the ambient. This means that if the multi-generation products of those compounds were observed in the ambient air, they should have been generated via a reaction that happened very recently."

and we have revised our supplement as:

"

Table S1. Summary of experimental conditions.

No.	Initial concentration of 1,3,5-TMB (ppb)	O_3 concentration (ppb)*	NO concentration (ppb)	NO_2 concentration (ppb)	Estimated OH exposure based on the precursor consumption ($\times10^{10}$ molecule cm^{-3} s)
1-1	54.6	451	0	0	1.85
1-2	58.9	455	0	0	1.12
1-3	62.7	467	0	0	0.52
1-4	38.4	434	0	0	4.40
1-5	39.9	441	0	0	4.09
1-6	41.2	445	0	0	3.48
1-7	41.9	453	0	0	2.87
1-8	43.8	461	0	0	2.19
1-9	45.6	471	0	0	1.33
1-10	46.8	479	0	0	0.63
1-11	47.7	483	0	0	0.59
1-12	48.1	482	0	0	4.49
1-13	48.4	427	0	0	3.98
1-14	47.8	434	0	0	3.59
1-15	47.9	443	0	0	3.15
1-16	48.9	451	0	0	2.68
1-17	49.5	458	0	0	1.89
1-18	49.7	467	0	0	1.13
1-19	50.3	480	0	0	0.53
1-20	28.9	428	0	0	4.87
1-21	31.3	428	0	0	4.81
1-22	32.5	429	0	0	4.41
1-23	33.4	440	0	0	3.81
1-24	33.9	448	0	0	3.25
1-25	34.4	455	0	0	2.38
1-26	34.8	466	0	0	1.61
1-27	49.7	424	0	0	4.19
1-28	50.6	434	0	0	3.78
1-29	50.0	441	0	0	3.43
1-30	50.5	448	0	0	2.97
1-31	51.4	457	0	0	2.44
1-32	51.6	464	0	0	1.78
1-33	52.5	477	0	0	1.06
1-34	46.6	429	0	0	4.35

1-35	47.3	436	0	0	3.85
1-36	47.9	442	0	0	3.52
1-37	48.8	451	0	0	3.01
1-38	50.0	460	0	0	2.56
1-39	50.6	466	0	0	1.81
1-40	51.6	477	0	0	1.16
1-41	29.7	864	2.01	60	3.11
1-42	37.1	856	1.85	64	2.89
1-43	44.6	853	1.86	67	2.73
1-44	52.3	854	1.76	68	2.57
1-45	59.7	856	1.71	70	2.41
1-46	67.8	858	1.65	71	2.26
1-47	26.8	860	1.96	65	3.19
1-48	31.5	874	1.93	68	3.09
1-49	39.4	874	1.84	70	2.86
1-50	46.7	879	1.76	72	2.70
1-51	55.3	881	1.70	73	2.53
1-52	64.8	880	1.63	74	2.36
1-53	73.3	864	1.61	75	2.19
1-54	84.1	883	1.57	78	2.06
1-55	29.2	714	4.81	104	3.98
1-56	35.5	703	4.82	111	3.77
1-57	16.7	695	5.32	109	4.18
1-58	22.9	697	5.21	112	4.14
1-59	29.6	699	4.91	117	3.84
1-60	36.0	698	4.70	119	3.62
1-61	41.4	698	4.52	122	3.43
1-62	46.5	688	4.61	128	3.31
1-63	52.4	692	4.47	130	3.18
1-64	25.0	675	5.46	125	3.89
1-65	30.9	683	5.32	127	3.68
1-66	36.8	688	5.02	131	3.47
1-67	42.3	688	4.89	132	3.33
1-68	48.5	688	4.64	134	3.22
2-1	30.8	147	0	0	0.55
2-2	30.8	151	0	0	0.24
2-3	30.8	152	0	0	0.10
2-4	30.8	152	0	0	0.06
2-5	34.5	123	7.11	38	0.31
2-6	34.5	137	3.10	21	0.20
2-7	34.5	144	1.30	11	0.09

** O_3 concentrations were stable values measured after the lights were turned on.

Table S4. Summary of radical concentrations estimated by the PAM_chem_v8 model in the 2nd-round experiments.

	Estimated [OH] with PAM_chem_v8 based on the precursor consumption ($\times 10^7$ molecule cm^{-3})	Estimated [HO_2] with PAM_chem_v8 based on the precursor consumption ($\times 10^8$ molecule cm^{-3})	Estimated [RO_2] with PAM_chem_v8 based on the precursor consumption ($\times 10^9$ molecule cm^{-3})
2-1	10.3	3.73	4.05
2-2	4.54	2.14	2.80
2-3	1.64	0.97	1.69

2-4	1.04	0.67	1.34
2-5	5.80	13.1	1.55
2-6	3.69	11.5	1.39
2-7	1.69	8.38	1.07

Table S6. The C9 and C18 products detected by nitrate CIMS in Exp.2-3. The exact mass is mass without adduct of a reagent ion of NO_3^-. "--" stands for the signal of compound was below the detection limit.

Molecular formula	Molar mass (Th)	Contributions to total C9 and C18 products in Exp. 2-3 (%)	Contributions to total C9 and C18 products in Exp. 2-4 (%)	DBE
$C_9H_{13}O_4$	247.0698	0.28	--	3.5
$C_9H_{14}O_4$	248.0776	0.34	--	3
$C_9H_{12}O_5$	262.0569	1.03	2.03	4
$C_9H_{13}O_5$	263.0647	0.36	--	3.5
$C_9H_{14}O_5$	264.0725	1.03	1.73	3
$C_9H_{12}O_6$	278.0518	1.60	2.45	4
$C_9H_{13}O_6$	279.0596	0.63	6.54	3.5
$C_9H_{14}O_6$	280.0674	4.64	2.11	3
$C_9H_{16}O_6$	282.0831	1.41	2.39	2
$C_9H_{10}O_7$	292.0310	1.17	2.40	5
$C_9H_{12}O_7$	294.0467	1.56	3.38	4
$C_9H_{13}O_7$	295.0545	2.34	6.74	3.5
$C_9H_{14}O_7$	296.0623	6.52	3.43	3
$C_9H_{15}O_7$	297.0701	4.15	1.73	2.5
$C_9H_{16}O_7$	298.0780	5.03	5.25	2
$C_9H_{12}O_8$	310.0416	3.20	3.31	4
$C_9H_{13}O_8$	311.0494	0.59	--	3.5
$C_9H_{14}O_8$	312.0572	3.39	4.42	3
$C_9H_{15}O_8$	313.0651	2.40	2.08	2.5
$C_9H_{16}O_8$	314.0729	7.31	8.70	2
$C_9H_{12}O_9$	326.0365	2.22	2.54	4
$C_9H_{13}O_9$	327.0443	1.30	1.52	3.5
$C_9H_{14}O_9$	328.0522	2.02	2.55	3
$C_9H_{15}O_9$	329.0600	0.78	--	2.5
$C_9H_{16}O_9$	330.0678	1.43	2.46	2
$C_9H_{12}O_{10}$	342.0314	1.61	1.83	4
$C_9H_{13}O_{10}$	343.0393	0.49	--	3.5
$C_9H_{14}O_{10}$	344.0471	1.07	--	3
$C_9H_{15}O_{10}$	345.0549	0.24	--	2.5
$C_9H_{16}O_{10}$	346.0627	0.37	--	2
$C_9H_{12}O_{11}$	358.0263	2.24	3.13	4
$C_9H_{13}O_{11}$	359.0342	0.60	--	3.5
$C_9H_{14}O_{11}$	360.0420	0.46	--	3
$C_9H_{15}O_{11}$	361.0498	0.19	--	2.5
$C_{18}H_{24}O_8$	430.1355	0.56	--	7
$C_{18}H_{26}O_8$	432.1511	4.83	5.86	6
$C_{18}H_{24}O_9$	446.1304	0.59	--	7
$C_{18}H_{26}O_9$	448.1461	1.35	2.53	6
$C_{18}H_{24}O_{10}$	462.1253	0.45	--	7
$C_{18}H_{25}O_{10}$	463.1332	0.36	--	6.5
$C_{18}H_{26}O_{10}$	464.1410	9.58	9.36	6
$C_{18}H_{28}O_{10}$	466.1566	2.97	2.42	5

$C_{18}H_{24}O_{11}$	478.1202	0.51	--	7
$C_{18}H_{26}O_{11}$	480.1359	2.28	2.15	6
$C_{18}H_{27}O_{11}$	481.1437	1.09	1.42	5.5
$C_{18}H_{28}O_{11}$	482.1515	2.44	1.70	5
$C_{18}H_{26}O_{12}$	496.1308	1.61	1.84	6
$C_{18}H_{28}O_{12}$	498.1465	1.13	--	5
$C_{18}H_{30}O_{12}$	500.1621	0.35	--	4
$C_{18}H_{24}O_{13}$	510.1101	0.33	--	7
$C_{18}H_{26}O_{13}$	512.1257	0.83	--	6
$C_{18}H_{27}O_{13}$	513.1335	0.51	--	5.5
$C_{18}H_{28}O_{13}$	514.1414	0.69	--	5
$C_{18}H_{30}O_{13}$	516.1570	0.33	--	4
$C_{18}H_{26}O_{14}$	528.1206	0.67	--	6
$C_{18}H_{27}O_{14}$	529.1284	0.17	--	5.5
$C_{18}H_{28}O_{14}$	530.1363	0.37	--	5
$C_{18}H_{30}O_{14}$	532.1519	0.30	--	4
$C_{18}H_{26}O_{15}$	544.1155	0.31	--	6
$C_{18}H_{27}O_{15}$	545.1234	0.24	--	5.5
$C_{18}H_{28}O_{15}$	546.1312	0.34	--	5
$C_{18}H_{30}O_{15}$	548.1469	0.21	--	4
$C_{18}H_{26}O_{16}$	560.1105	0.30	--	6
$C_{18}H_{28}O_{16}$	562.1261	0.30	--	5

Table S7. The C9 products detected by nitrate CIMS in Exp.2-7.

Molecular formula	Molar mass (Th)	Contributions to total C9 and C18 products signals (%)	DBE
$C_9H_{12}O_6$	216.0634	1.25	4
$C_9H_{13}O_6$	217.0712	1.98	3.5
$C_9H_{14}O_6$	218.0790	1.95	3
$C_9H_{13}NO_6$	231.0743	3.97	3
$C_9H_{12}O_7$	232.0583	1.59	4
$C_9H_{13}O_7$	233.0661	2.92	3.5
$C_9H_{15}O_7$	235.0818	0.97	2.5
$C_9H_{13}NO_7$	247.0692	9.32	3
$C_9H_{12}O_8$	248.0532	3.11	4
$C_9H_{13}O_8$	249.0610	0.94	3.5
$C_9H_{14}O_8$	250.0689	2.15	3
$C_9H_{13}NO_8$	263.0641	21.25	3
$C_9H_{13}O_9$	265.0559	1.57	3.5
$C_9H_{15}NO_8$	265.0798	2.94	2
$C_9H_{13}NO_9$	279.0590	5.45	3
$C_9H_{12}O_{10}$	280.0430	1.91	4
$C_9H_{14}NO_9$	280.0669	3.34	2.5
$C_9H_{13}O_{10}$	281.0509	1.52	3.5
$C_9H_{15}NO_9$	281.0747	2.51	2
$C_9H_{14}N_2O_9$	294.0699	1.76	2
$C_9H_{13}NO_{10}$	295.0539	3.52	3
$C_9H_{14}N_2O_{10}$	310.0649	18.15	2
$C_9H_{13}NO_{11}$	311.0489	3.11	3
$C_9H_{12}N_2O_{11}$	324.0441	1.23	3
$C_9H_{14}N_2O_{11}$	326.0598	1.60	2

Also, I would advise the authors to be careful what they consider as an "ORF setup". It seems they have considered OFR to be everything where oxidation is studied, notwithstanding that several other setups have been previously meticulously characterized and assigned as well controlled flow reactors and environmental chambers that aim to investigate the processes under ambient relevant conditions. Especially the setups mentioned in the response letter, the Jülich JPAC chambers and the very carefully controlled free-jet flow reactor of Torsten Berndt in TROPOS, Leipzig. In JPAC (e.g., Garmash et al., 2020) the reaction time is much larger (ca. 50 minutes), surface-to-volume smaller and the oxidation mixture more dilute, leading to more ambient relevant conditions. In TROPOS (e.g., Wang et al., 2017) the reactions have been studied in short reaction times (at 7.9 s) in a practically wall-less setup with careful control over the reagent concentrations. Equating these setups and works with the PAM and the current work appears wrong.

R2. We believe that in this comment the reviewer concerns about the usage/definition of PAM as an oxidation flow reactor (OFR). OFR is defined by the community as "flow reactors using oxidants with substantially (often orders of magnitude) higher concentrations than in the atmosphere to accelerate the oxidation chemistry in them" (Peng and Jimenez, 2020). The key aspects for an OFR are the flowing reaction manner of oxidation reactions and the higher concentrations of oxidants to accelerate oxidation reactions inside the reactor, which a PAM fulfills. In fact, the PAM manufactured by Aerodyne Research Inc. or flow reactors constructed with the same settings has been considered as an OFR by various groups for a long period of time (Avery et al., 2023; Lambe et al., 2011, 2015, 2017, 2019; Peng et al., 2015, 2016, 2018; Li et al., 2015; Kang et al., 2007; Watne et al., 2018). Meanwhile, our new experiments have shown that PAM can be used to study reactions under chemical regimes with atmospheric relevant [OH], i.e., 10^7 cm^{-3}, but the total OH exposure in the flow tube under this condition is limited because of the pre-determined residence time in the PAM.

Nevertheless, if one is interested in reactions with extended OH exposures that is not straightforward to the current chamber/flow tube techniques, a possible solution is to increase [OH] to compensate for the residence time. As the reviewer has pointed out, one should be very careful with the obtained results because the unequally scaled radical concentrations and/or condensation of low-volatile products can both alter the product distribution even the production or not of a particular product. This is also why the concerns on the atmospheric relevance of chemistry in the OFR has persisted (Peng and Jimenez, 2020).

Although whether PAM can be considered as an OFR or not is absolutely relevant, the more important issue is whether results from this study is relevant to the ambient or used to help understand multigeneration oxidation mechanisms of aromatics and their stabilized products, which, we believe, is elaborated in **R1** of this reply and Session 3.1 of the revised manuscript (version R2).

The chosen autoxidation rate of 7 s^{-1} is very high, and not supported by the referenced study. The Authors state they based this on the expected autoxidation rate of ethylbenzene, yet this higher rate in the referenced work is due to a secondary hydrogen on the ethyl substituent, which is absent from methyl groups in the studied TMB molecule. Instead, the autoxidation rate from a methyl group was found 270 times slower (7 s^{-1} / 0.026 s^{-1}). If one takes into account the symmetry with three methyl groups, then on could expect the 1,3,5-TMB rate as around 3 times higher, yet still likely less than 0.1 s^{-1}. Thus, this choice necessarily leads to severely overestimated fraction of autoxidized products. In fact, the Authors even state that "We arbitrarily set the autoxidation reaction rate…", and this seems to be critical for the analysis, leading to conclusion that 81% to 89.7% of the reaction products are due to autoxidation.

R3. We follow quantum calculation results on the autoxidation reaction of a methyl group adjacent to the RO_2 functionality group (Wang et al. 2017), and time the suggested rate (0.026 s^{-1}) by 3 due to the symmetry with three methyl groups in our parent compound. The obtained autoxidation reaction rate is 0.078 s^{-1}, which has been updated in our PAM_chem_v8 model. The updated autoxidation reaction rate leads to changes in the calculated concentrations of BPR and $C_9H_{13}O_7$·, but almost does not impact the sum of [RO_2]. Given an uncertainty range of 1 order magnitude for the autoxidation rate (Wang et al. 2017) that covers 0.0078 – 0.78 s^{-1}, the total [RO_2] estimated by the model would vary by less than 2% even under the highest [OH] level.

The selection of this autoxidation rate is now updated in Section S1.

In addition, due to the update of the autoxidation rate, radical concentrations in the high [OH] experiments and radical profiles in Fig. S1 are updated.

Discussions on the 1st-round experiments have also been updated, which has been included in **R1.2**.

We have revised our manuscript (Line 329 - 339), which reads,

Concentration profiles of OH, RO_2, and HO_2 as a function of OH exposures in our high [OH] experiments without NO_x, i.e., the 1st-round experiments, are illustrated in Fig. S1a. According to the modified PAM_chem_v8, when [OH] increased from 9.32×10^7 to 1.03×10^9 molecule cm^{-3}, [HO_2] increased from 7.25×10^8 to 2.79×10^9 molecule cm^{-3}, whereas [RO_2] concentrations increased from 5.17×10^9 to 9.5×10^9 molecule cm^{-3}. The radical concentrations in high [OH] experiments with NO_x (Fig. S1b) varied in a similar range, with [RO_2] ranging from 4.38×10^9 to 9.13×10^9 molecule cm^{-3}, HO_2 ranging from 4.47×10^9 to 6.47×10^9 molecule cm^{-3}, and OH ranging from 3.86×10^8 to 7.82×10^8 molecule cm^{-3}, respectively. The ratios between HO_2/OH and RO_2/OH in the 1st-round experiments were generally in the same order of magnitude with the ambient atmosphere (Whalley et al., 2021).

We have revised Supplementary Text S1, which reads,

"We follow quantum calculation results on the autoxidation reaction of a methyl group adjacent to the RO_2 functionality group (Wang et al. 2017), and time the suggested rate (0.026 s^{-1}) by 3 due to the symmetry with three methyl groups in our parent compound. The obtained autoxidation reaction rate is 0.078 s^{-1}.

"

We have revised Figure S1, which is shown below

(a)

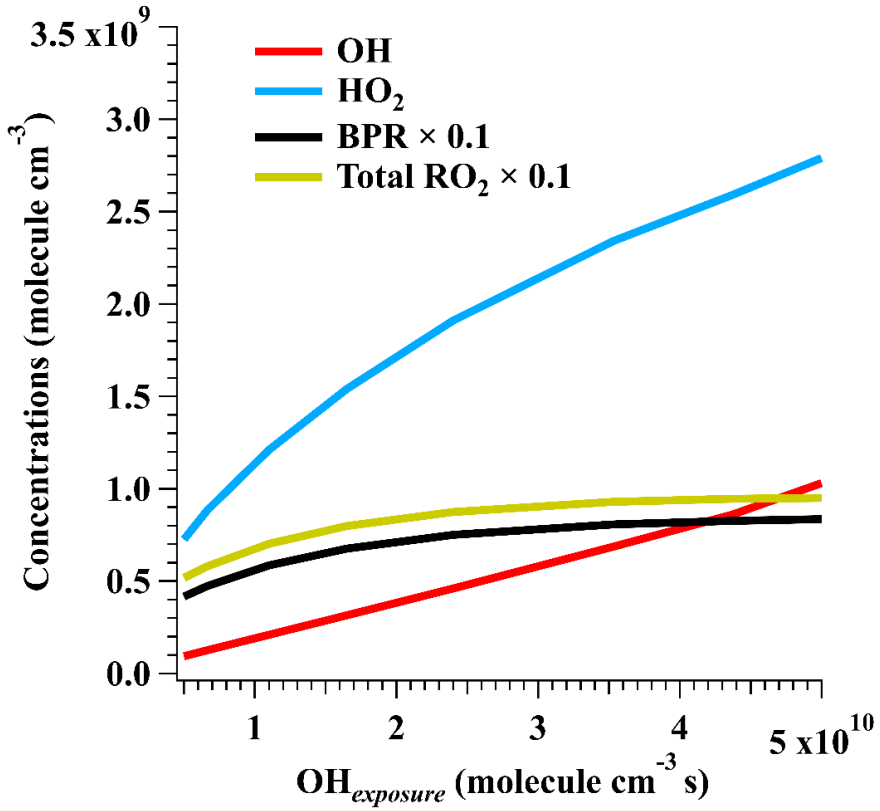

(b)

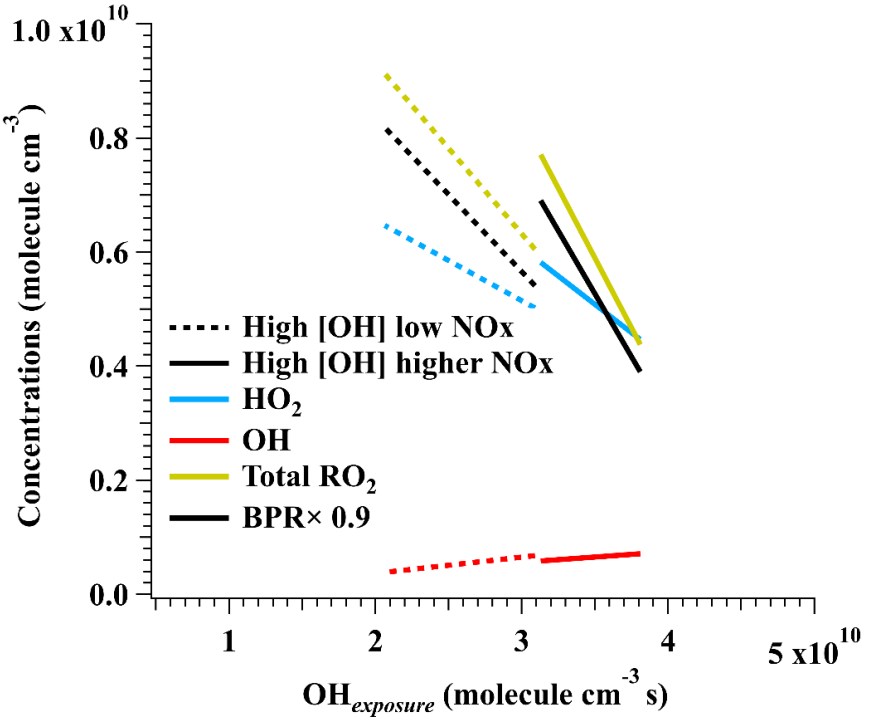

Figure S1. (a) Concentration profiles of OH, HO_2, BPR, and total RO_2 in the 1st-round experiments in absent of NO_x in the PAM OFR as a function of OH exposures. The average total concentrations of RO_2 and BPR were scaled with a factor of 0.1 for a better visualization. (b) Concentration profiles of OH, HO_2, BPR, and total RO_2 in the 1st-round experiments in presence of NO_x in the PAM OFR as a function of OH exposures. The average total concentrations of RO_2 were scaled with a factor of 0.9 for a better visualization.

Similarly, as the pool of simulated RO2 consists only of the two prominent RO2 radicals (i.e., BPR and C9H13O7) which both have been assigned with a very high accretion rate, and then the whole pool of ROOR is counted based on these same two radicals. That would also seem to indicate an overestimated importance for the accretion reaction, or do I read it wrong?

R4. Indeed, more RO_2 radicals than the two (BPR and $C_9H_{13}O_7$·) currently explicitly mentioned and modeled exist in the PAM OFR tube, which come from the subsequent fragmentation of stabilized products as suggested by MCM and the multi-generation OH oxidation of stabilized products.

Accretion reaction rate constants for smaller RO_2 generated by the fragmentation of stabilized products are typically 1 - 2 orders of magnitude lower than those of BPR and $C_9H_{13}O_7$·, as suggested in a previous study (Berndt et al., 2018). Accretion reaction rate constants of multi-generation RO_2 are currently unknown, but should be at least no lower than that of the smaller RO_2. However, reactions of these two categories of RO_2 with BPR and $C_9H_{13}O_7$·, including RO_2 termination reactions (R1 – R3) and accretion reactions (R4), were not included in the model. Therefore, it is likely that the accretion channel of BPR and $C_9H_{13}O_7$· was not overestimated but underestimated.

PAM_chem_v8 model simulations here are conducted to characterize [OH], [HO_2], and [RO_2] inside the PAM OFR, not to really capture the detailed reactions, including the fragmentation, re-initiation of OH oxidation, and other chemical reactions. This model was developed to specifically simulate the formation and evolution of key radicals and oxidants, and quantify the radical budget for the OFR (Li et al., 2015). On the other hand, detailed reaction mechanisms e.g., the MCM-based 0-D box model, are still unlikely to estimate the exact significance of accretion reactions in the PAM OFR, as they do not cover RO_2 generated in the re-initiation of OH oxidation, whose interactions with BPR and $C_9H_{13}O_7$· are obviously unignorable based on our observations in both rounds of experiments.

The accretion reactions in the PAM have already been intensified a lot due to the much more abundant BPR and $C_9H_{13}O_7$· than those in the ambient. Therefore, the conclusion drawn from the high [OH] experiments is constrained to the proximity of monomeric termination products to those under ambient conditions as stated in **R1**. We focus on the monomeric reaction of RO_2 in the PAM OFR, and agree that the accretion reaction (*R*4) works as a magnified pathway of RO_2 in the laboratory. The HOM dimer data obtained from the high [OH] experiments serve as a symbolic illustration of the enhanced abundance of multi-generation OH oxidation in the laboratory, correlating with the elevated levels of radicals in the reactor. The uncertainty in the proportions of accretion reactions would not impact the existence of multi-generation OH oxidation.

Furthermore, I still find the decreasing ROOR signal problematic, as under such short timescales it would seem to indicate either particle formation, or secondary reactions of the formed ROOR, neither which would be expected under atmospheric conditions at such short times. It is stated that no particle formation was observed with long SMPS, but I suppose the SMPS cut-off limit is so high that it would not see the fresh particles in any case. Or what was the smallest measurable particle size with the SMPS system?

R5. The secondary oxidation of HOM dimers absolutely happened in the PAM OFR in both the 1st-round and the 2nd-round experiments, and their physical loss due to the generation of particles might have happened, too.

The long SMPS consisted of a long-DMA (TSI model 3081) and a CPC (TSI model 3787), covering a particle number size distribution from 13.6 nm to 736.5 nm. As suggested by the reviewer, the long SMPS cannot measure freshly formed particles. Thus, though not detected in this study, we cannot absolutely deny

the possibility that particles might have been generated with the increment of OH exposures, resulting in a larger physical loss of HOMs. We would like to add this information into the revised manuscript.

If the survival time permits, the secondary OH oxidation of stabilized HOM dimers should be feasible and the reaction rate constant should be at least comparable to those stabilized monomers. According to the general mechanisms of OH addition reactions to a C=C bond, the resulting RO_2 radical possesses one more hydrogen atom and three more oxygen atoms than the reactants. Then the most abundant dimer radical, $C_{18}H_{27}O_{11}$· (Figure R4), and the second most one, $C_{18}H_{27}O_{13}$·, in the atmospheric relevant [OH] experiment of Exp. 2-3 exactly correspond to two previous reported HOM dimer products $C_{18}H_{26}O_8$ and $C_{18}H_{26}O_{10}$ (Berndt et al., 2018), respectively, which confirms the secondary OH oxidation of stabilized HOM dimers, though in Exp. 2-4 only $C_{18}H_{27}O_{11}$· was detected.

In the ambient, pre-existing particles can contribute to the physical loss of oxidation products. Atmospheric [OH] can also re-initiate secondary OH oxidation reactions. Nevertheless, the detailed timescale for the decrease of dimers should be different from what we have observed in the laboratory due to the complex environment in the ambient.

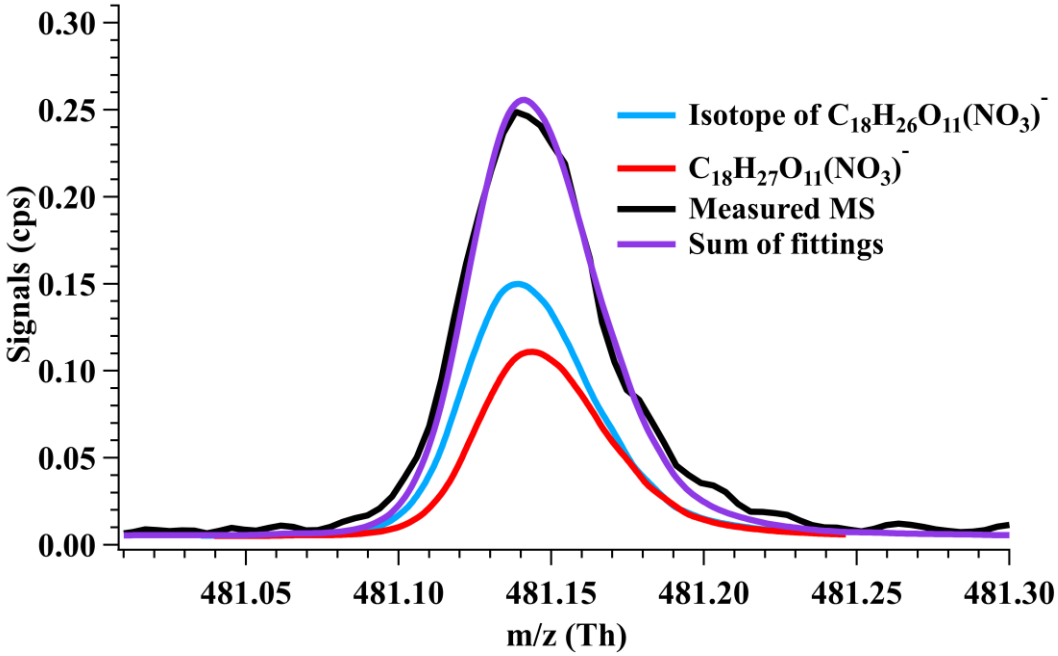

Figure R4. The fitting of averaged $C_{18}H_{27}O_{11}(NO_3)^-$ measured by nitrate CIMS in the Experiment 2-3 and 2-4.

We have revised our manuscript (Line 755 - 761), which reads,

"With the decrease of particulate pollution and thus condensation sinks in the polluted areas, the physical loss of HOMs might be lower and the chemical process can be more important. This series of experiments are not meant to specifically find out the detailed OH exposures when the maximum concentrations of HOM dimers will occur, but try to indicate how HOM dimers evolve with the increase of OH exposures. This work can be regarded as an indicator for the potential chemical fates of HOM dimers in the atmosphere if their survival time permitted."

We have revised our supplementary Text S1, which reads,

"In our experiments, measurement results by a long-SMPS show that the aerosol particles presented in the PAM OFR were few. The long SMPS consisted of a long-DMA (TSI model 3081) and a CPC (TSI model 3787), covering a particle number size distribution from 13.6 nm to 736.5 nm. Thus, though not detected in this study, we cannot absolutely deny the possibility that particles might have been generated with the increment of OH exposures, resulting in a larger physical loss of HOMs. This part of physical loss might be underestimated."

The Authors seem to several times make the claim that the OH concentration in the work of Garmash et al., was higher, which is not the case. Even the highest [OH] = 4.5 x 10^8 cm^-3 was still considerably smaller than reported in the current study (i.e., 1.5 10^9 cm^-3). Moreover, in the work of Garmash et al., it was recognized that with such an unrealistically high OH, you can't really derive sound mechanistic conclusions, and thus no mechanisms were proposed. However, the fact that the rate coefficients increase together with the number of OH substituents was recognized during the study, which is why the potential for "multi-generation OH oxidation" in product formation was acknowledged as a complication for data analysis, and no other mechanistic description was provided due to the non-conventional reaction conditions.

This comparison seems in any case problematic, as the Authors talk about 0.7-6.9 hours of atmospheric aging at 2x10^6 cm^-3 [OH], yet the residence time in the setup is only 53 seconds. The exact [OH] used seemed to be unknown, yet with the response letter the Authors quote an OH concentration of 1.5x10^9 cm^-3. Now, in Garmash et al., the residence time is roughly 60 times longer and the maximum used [OH] is 4.5x10^8 cm^-3, naturally leading to longer aging timescale. What the Authors seem to miss here is that what is more important is the absolute concentrations of the reagents, as they push the chemistry to an unrealistic regime, and not the equivalent dose. And repeating from above, Garmash et al., did not derive mechanistic conclusion from the higher [OH] experiments, other than the sequential oxidation behavior.

R6. Sorry for the unclarity in the previous comparison with the Garmash et al. study (2020). We agree with the reviewer that one should be very careful with the obtained results under laboratory high [OH] conditions because the unequally scaled radical concentrations and/or condensation of low-volatile products can both alter the product distribution even the production or not of a particular product.

Nevertheless, OFR methods provide an opportunity to investigate oxidation reactions with short residence times and reduced wall effects. Despite these advantages of OFR, concerns over the atmospheric relevance of the radical chemistry (and hence gas and aerosol products) in OFR have persisted.

Based on our previous analysis on the radical concentrations of high [OH] experiments, the product distributions of RO_2 monomeric termination reactions in the PAM are atmospheric relevant. We were trying to show that the subsequent oxidation reactions do exist for stabilized oxidation products of TMB, which could be deduced based on the DBE of detected compounds. Once a re-initiated OH oxidation of these first-generation products happened, we can unambiguously detect the secondary reaction based on the lower DBE of the secondary product. Besides, the comparison between the high [OH] experiments and the newly conducted low [OH] experiments confirms that these low DBE products are related to the increasing [OH].

Certainly, based on these results we cannot make conclusions that re-initiated OH oxidation of a certain compound in the ambient can be as important as in the lab, because of the different survival time, as discussed in **R1**.

We acknowledge that the mechanistic conclusion obtained in our high [OH] experiments is not robust enough by themselves, as the ratio of radicals will impact the distribution of products. Fortunately, in the laboratory low [OH] experiments, we still detected the low DBE products and critical radicals, i.e., $C_9H_{15}O_8$·

and $C_9H_{15}O_9$·, which are discussed in the proposed schemes (Scheme 2 and Scheme 3). This confirms that these reactions can happen and are still important in the atmospheric relevant [OH] conditions. Please refer to **R1.2**.

So, my problem with the current documentation is that PAM, and the OFR approach, is really a methodology for reaching emission regulations, but it's ill-suited for detailing complex chemistry under atmospheric relevant concentration regimes. It would make an interesting comparison to see how the products change between atmospheric 10^6 to 10^7 cm^{-3} to OFR 10^{-9} cm^{-3}, but unfortunately such an analysis was not provided. (To put it another way, if you would have written the story like "if HOMs would survive a day – what would happen", and not trying to insist this is strictly atmospherically relevant product distribution, then this would have made much more sense).

R7. We acknowledge that the issue with high [OH] experiments lies in the scaling of certain reaction pathways to unrealistic levels, thereby facilitating the observation of reaction pathways that are minor in the ambient. Because of the limited survival time of reactants and competition of various reaction channels, laboratory products won't be identical to ambient ones after the same OH exposures. Even the same product can be generated in both the laboratory and the ambient, the relative significance of this products is not likely to be the same.

We agree that experiments under atmospheric radical concentrations are meaningful and helpful to probe the existence of certain oxidation reactions in the real atmosphere. Therefore, these atmospheric relevant [OH] experiments have been conducted, whose results and discussions are provided in **R1**.

We now discuss the chemical regimes for the investigated low [OH] experiments and show that the physical loss was biased to be lower in the PAM. Please refer to **R1.4**.

Also, the Authors probably slightly misunderstood my comment about the potential influence of light: It would be expected to be a problem for the aromatic oxidation products undergoing photo-oxidation, not that the precursor TMB would be photolyzed. Also, I don't understand the comment that says: "Meanwhile, photolysis of HOMs can lead to decomposition, decreasing detected signals of HOMs, but unlikely to generate new HOMs." If the photolysis yields radical intermediates, as it does, then these new intermediates can continue oxidation to HOM as well. It's quite likely that this was occurring in the experiments.

R8. We separated the influences of photolysis into two paragraphs, one on the precursors (**Line 177 - 184** in the previous revised manuscript with marks) and the other one on the oxidation products (**Line 185 - 189** in the previous revised manuscript with marks).

Since the photo intensity of 254 nm lamps can be estimated with the PAM_chem_v8 model, we can calculate the OH reaction rate and the photolysis rate of stabilized HOMs in the OFR, which together show that the proportion of photolysis was quite low. The calculations have been provided in the last reply.

On the other hand, according to the MCM (Saunders et al., 2003), the photolysis of oxygenated organic compounds, e.g. benzaldehyde, other complex carbonyl compounds, and hydroperoxides, will decompose the C-C bond adjacent to the oxygenated functionality. In the last version, we were trying to state that the photolysis, if really occurred, would mainly result in the decomposition of HOMs and generation of new compounds with fewer carbon atoms. In other words, photolysis is unlikely to diversify or augment the detected HOMs with 9 or 18 carbon atoms, which are the main subject of discussion of this paper. We are

sorry we did not clarity our discussion as C9 or C18 HOMs in **Line 185 - 189** in the previous revised manuscript with marks.

We have revised our manuscript (Line 193 - 207), which reads,

"Non-tropospheric VOC and OVOC photolysis is a typical issue that should be taken into account when evaluating the settings of OFR laboratory experiments, especially in the high UV light dose settings in the 1st-round experiments. Photolysis of the precursor and HOMs were evaluated, showing that photolysis was not a contributor to our observation. The photolysis rate of 1,3,5-TMB can be estimated based on the absorption cross-sections of 1,3,5-TMB at 254 nm (Keller-Rudek et al., 2013) and UV photon fluxes estimated by a chemistry model discussed in the following sections. The ratio of photolysis-to-OH reaction in our 1st-round experiments was merely 0.010 – 0.033. Hence, photolysis of 1,3,5-TMB was insignificant in the OFR. For stabilized products such as C9 and C18 HOMs, the cross sections of organic molecules are usually ~ 3.9×10^{-18} - 3.9×10^{-17} cm^2 (Peng et al., 2016), while the reaction rate between OH and the stabilized first-generation products are estimated to be around 1.28×10^{-10} $molecule^{-1}$ cm^3 s^{-1}, as suggested by MCM (Jenkin et al., 2003). Hence, the ratio of photolysis rates of C9 and C18 HOMs to their secondary OH oxidation rates is estimated to be merely around 0.020 – 0.056 in the 1st-round experiments. In the 2nd-round, the influences of photolysis should be even lower due to the much lower light intensity."

Thanks for educating me that in PAM a ¼" Teflon tube is used. This is not adequate for measuring very condensable products. This is a problem I had overlooked in the common PAM methodology.

R9. As stated in the **R1**, we have modified the sampling system of PAM OFR. A 30 cm-long Teflon tube with a 1/2 in. OD was utilized for the sampling of the new nitrate CI-TOF. Several new low volatile species have been detected in the 2nd-round experiments, i.e., $C_9H_xO_{11}$ (x = 12 - 15).

Reviewer #2*: Wang et al. present laboratory results where they oxidized trimethylbenzene to investigate the role of autoxidation. The authors have done an exemplary job responding to both reviewers' comments, providing much needed calculations to indicate how their observations are similar to atmospheric conditions, softening the language when necessary, and improving the figures and story overall. The paper is ready for consideration for publication in ACP.*

We thank this reviewer for his/her positive view on our manuscript.

References

Avery, A. M., Alton, M. W., Canagaratna, M. R., Krechmer, J. E., Sueper, D. T., Bhattacharyya, N., Hildebrandt Ruiz, L., Brune, W. H., and Lambe, A. T.: Comparison of the Yield and Chemical Composition of Secondary Organic Aerosol Generated from the OH and Cl Oxidation of Decamethylcyclopentasiloxane, ACS Earth Sp. Chem., 7, 218–229, https://doi.org/10.1021/acsearthspacechem.2c00304, 2023.

Berndt, T., Scholz, W., Mentler, B., Fischer, L., Herrmann, H., Kulmala, M., and Hansel, A.: Accretion Product Formation from Self- and Cross-Reactions of RO2 Radicals in the Atmosphere, Angew. Chemie - Int. Ed., 57, 3820–3824, https://doi.org/10.1002/anie.201710989, 2018.

Bianchi, F., Kurtén, T., Riva, M., Mohr, C., Rissanen, M. P., Roldin, P., Berndt, T., Crounse, J. D., Wennberg, P. O., Mentel, T. F., Wildt, J., Junninen, H., Jokinen, T., Kulmala, M., Worsnop, D. R., Thornton, J. A., Donahue, N., Kjaergaard, H. G., and Ehn, M.: Highly Oxygenated Organic Molecules (HOM) from Gas-Phase Autoxidation Involving Peroxy Radicals: A Key Contributor to Atmospheric Aerosol, Chem. Rev., 119, 3472–3509, https://doi.org/10.1021/acs.chemrev.8b00395, 2019.

Deng, C., Fu, Y., Dada, L., Yan, C., Cai, R., Yang, D., Zhou, Y., Yin, R., Lu, Y., Li, X., Qiao, X., Fan, X., Nie, W., Kontkanen, J., Kangasluoma, J., Chu, B., Ding, A., Kerminen, V. M., Paasonen, P., Worsnop, D. R., Bianchi, F., Liu, Y., Zheng, J., Wang, L., Kulmala, M., and Jiang, J.: Seasonal characteristics of new particle formation and growth in urban Beijing, Environ. Sci. Technol., 54, 8547–8557, https://doi.org/10.1021/acs.est.0c00808, 2020.

Ehn, M., Thornton, J. A., Kleist, E., Sipilä, M., Junninen, H., Pullinen, I., Springer, M., Rubach, F., Tillmann, R., Lee, B., Lopez-Hilfiker, F., Andres, S., Acir, I. H., Rissanen, M., Jokinen, T., Schobesberger, S., Kangasluoma, J., Kontkanen, J., Nieminen, T., Kurtén, T., Nielsen, L. B., Jørgensen, S., Kjaergaard, H. G., Canagaratna, M., Maso, M. D., Berndt, T., Petäjä, T., Wahner, A., Kerminen, V. M., Kulmala, M., Worsnop, D. R., Wildt, J., and Mentel, T. F.: A large source of low-volatility secondary organic aerosol, Nature, 506, 476–479, https://doi.org/10.1038/nature13032, 2014.

Eisele, F. L. and Tanner, D. J.: Measurement of the gas phase concentration of H 2 SO 4 and methane sulfonic acid and estimates of H 2 SO 4 production and loss in the atmosphere, J. Geophys. Res. Atmos., 98, 9001–9010, https://doi.org/10.1029/93JD00031, 1993.

Garmash, O., Rissanen, M. P., Pullinen, I., Schmitt, S., Kausiala, O., Tillmann, R., Zhao, D., Percival, C., Bannan, T. J., Priestley, M., Hallquist, Å. M., Kleist, E., Kiendler-Scharr, A., Hallquist, M., Berndt, T., McFiggans, G., Wildt, J., Mentel, T. F., and Ehn, M.: Multi-generation OH oxidation as a source for highly oxygenated organic molecules from aromatics, Atmos. Chem. Phys., 20, 515–537, https://doi.org/10.5194/acp-20-515-2020, 2020.

Guo, Y., Yan, C., Liu, Y., Qiao, X., Zheng, F., Zhang, Y., Zhou, Y., Li, C., Fan, X., Lin, Z., Feng, Z., Zhang, Y., Zheng, P., Tian, L., Nie, W., Wang, Z., Huang, D., Daellenbach, K. R., Yao, L., Dada, L., Bianchi, F., Jiang, J., Liu, Y., Kerminen, V. M., and Kulmala, M.: Seasonal variation in oxygenated organic molecules in urban Beijing and their contribution to secondary organic aerosol, Atmos. Chem. Phys., 22, 10077–10097, https://doi.org/10.5194/acp-22-10077-2022, 2022.

Jenkin, M. E., Saunders, S. M., Wagner, V., and Pilling, M. J.: Protocol for the development of the Master Chemical Mechanism, MCM v3 (Part B): tropospheric degradation of aromatic volatile organic compounds, Atmos. Chem. Phys., 3, 181–193, https://doi.org/10.5194/acp-3-181-2003, 2003.

Kang, E., Root, M. J., Toohey, D. W., and Brune, W. H.: Introducing the concept of Potential Aerosol Mass (PAM), Atmos. Chem. Phys. Atmos. Chem. Phys., 7, 5727–5744, 2007.

Keller-Rudek, H., Moortgat, G. K., Sander, R., and Sörensen, R.: The MPI-Mainz UV/VIS spectral atlas of gaseous molecules of atmospheric interest, Earth Syst. Sci. Data, 5, 365–373, https://doi.org/10.5194/essd-5-

365-2013, 2013.
Krechmer, J., Lopez-Hilfiker, F., Koss, A., Hutterli, M., Stoermer, C., Deming, B., Kimmel, J., Warneke, C., Holzinger, R., Jayne, J., Worsnop, D., Fuhrer, K., Gonin, M., and De Gouw, J.: Evaluation of a New Reagent-Ion Source and Focusing Ion− Molecule Reactor for Use in Proton-Transfer-Reaction Mass Spectrometry, Anal. Chem., 90, 12011–12018, https://doi.org/10.1021/acs.analchem.8b02641, 2018.
Lambe, A., Massoli, P., Zhang, X., Canagaratna, M., Nowak, J., Daube, C., Yan, C., Nie, W., Onasch, T., Jayne, J., Kolb, C., Davidovits, P., Worsnop, D., and Brune, W.: Controlled nitric oxide production via O(1D) + N2O reactions for use in oxidation flow reactor studies, Atmos. Meas. Tech., 10, 2283–2298, https://doi.org/10.5194/amt-10-2283-2017, 2017.
Lambe, A. T., Ahern, A. T., Williams, L. R., Slowik, J. G., Wong, J. P. S., Abbatt, J. P. D., Brune, W. H., Ng, N. L., Wright, J. P., Croasdale, D. R., Worsnop, D. R., Davidovits, P., and Onasch, T. B.: Characterization of aerosol photooxidation flow reactors: heterogeneous oxidation, secondary organic aerosol formation and cloud condensation nuclei activity measurements, Atmos. Meas. Tech, 4, 445–461, https://doi.org/10.5194/amt-4-445-2011, 2011.
Lambe, A. T., Chhabra, P. S., Onasch, T. B., Brune, W. H., Hunter, J. F., Kroll, J. H., Cummings, M. J., Brogan, J. F., Parmar, Y., Worsnop, D. R., Kolb, C. E., and Davidovits, P.: Effect of oxidant concentration, exposure time, and seed particles on secondary organic aerosol chemical composition and yield, Atmos. Chem. Phys., 15, 3063–3075, https://doi.org/10.5194/acp-15-3063-2015, 2015.
Lambe, A. T., Krechmer, J. E., Peng, Z., Casar, J. R., Carrasquillo, A. J., Raff, J. D., Jimenez, J. L., and Worsnop, D. R.: HOx and NOx production in oxidation flow reactors via photolysis of isopropyl nitrite, isopropyl nitrite-d7 and 1,3-propyl dinitrite at λ = 254, 350, and 369 nm, Atmos. Meas. Tech., 12, 299–311, https://doi.org/10.5194/amt-12-299-2019, 2019.
Li, R., Palm, B. B., Ortega, A. M., Hlywiak, J., Hu, W., Peng, Z., Day, D. A., Knote, C., Brune, W. H., De Gouw, J. A., and Jimenez, J. L.: Modeling the radical chemistry in an oxidation flow reactor: Radical formation and recycling, sensitivities, and the OH exposure estimation equation, J. Phys. Chem. A, 119, 4418–4432, https://doi.org/10.1021/jp509534k, 2015.
Lu, K. D., Rohrer, F., Holland, F., Fuchs, H., Bohn, B., Brauers, T., Chang, C. C., Häseler, R., Hu, M., Kita, K., Kondo, Y., Li, X., Lou, S. R., Nehr, S., Shao, M., Zeng, L. M., Wahner, A., Zhang, Y. H., and Hofzumahaus, A.: Observation and modelling of OH and HO2 concentrations in the Pearl River Delta 2006: A missing OH source in a VOC rich atmosphere, Atmos. Chem. Phys., 12, 1541–1569, https://doi.org/10.5194/acp-12-1541-2012, 2012.
Ma, X., Tan, Z., Lu, K., Yang, X., Chen, X., Wang, H., Chen, S., Fang, X., Li, S., Li, X., Liu, J., Liu, Y., Lou, S., Qiu, W., Wang, H., Zeng, L., and Zhang, Y.: OH and HO2 radical chemistry at a suburban site during the EXPLORE-YRD campaign in 2018, Atmos. Chem. Phys., 22, 7005–7028, https://doi.org/10.5194/acp-22-7005-2022, 2022.
Peng, Z. and Jimenez, J. L.: Radical chemistry in oxidation flow reactors for atmospheric chemistry research, Chem. Soc. Rev., 49, 2570–2616, https://doi.org/10.1039/c9cs00766k, 2020.
Peng, Z., Day, D. A., Stark, H., Li, R., Lee-Taylor, J., Palm, B. B., Brune, W. H., and Jimenez, J. L.: HO x radical chemistry in oxidation flow reactors with low-pressure mercury lamps systematically examined by modeling, Atmos. Meas. Tech, 8, 4863–4890, https://doi.org/10.5194/amt-8-4863-2015, 2015.
Peng, Z., Day, D. A., Ortega, A. M., Palm, B. B., Hu, W., Stark, H., Li, R., Tsigaridis, K., Brune, W. H., and Jimenez, J. L.: Non-OH chemistry in oxidation flow reactors for the study of atmospheric chemistry systematically examined by modeling, Atmos. Chem. Phys., 16, 4283–4305, https://doi.org/10.5194/acp-16-4283-2016, 2016.

Peng, Z., Palm, B. B., Day, D. A., Talukdar, R. K., Hu, W., Lambe, A. T., Brune, W. H., and Jimenez, J. L.: Model Evaluation of New Techniques for Maintaining High-NO Conditions in Oxidation Flow Reactors for the Study of OH-Initiated Atmospheric Chemistry, ACS Earth Sp. Chem., 2, 72–86, https://doi.org/10.1021/acsearthspacechem.7b00070, 2018.
Saunders, S. M., Jenkin, M. E., Derwent, R. G., and Pilling, M. J.: Protocol for the development of the Master Chemical Mechanism, MCM v3 (Part A): Tropospheric degradation of non-aromatic volatile organic compounds, Atmos. Chem. Phys., 3, 161–180, https://doi.org/10.5194/acp-3-161-2003, 2003.
Tan, Z., Fuchs, H., Lu, K., Hofzumahaus, A., Bohn, B., Broch, S., Dong, H., Gomm, S., Häseler, R., He, L., Holland, F., Li, X., Liu, Y., Lu, S., Rohrer, F., Shao, M., Wang, B., Wang, M., Wu, Y., Zeng, L., Zhang, Y., Wahner, A., and Zhang, Y.: Radical chemistry at a rural site (Wangdu) in the North China Plain: Observation and model calculations of OH, HO2 and RO2 radicals, Atmos. Chem. Phys., 17, 663–690, https://doi.org/10.5194/acp-17-663-2017, 2017.
Tan, Z., Rohrer, F., Lu, K., Ma, X., Bohn, B., Broch, S., Dong, H., Fuchs, H., Gkatzelis, G. I., Hofzumahaus, A., Holland, F., Li, X., Liu, Y., Liu, Y., Novelli, A., Shao, M., Wang, H., Wu, Y., Zeng, L., Hu, M., Kiendler-Scharr, A., Wahner, A., and Zhang, Y.: Wintertime photochemistry in Beijing: Observations of ROx radical concentrations in the North China Plain during the BEST-ONE campaign, Atmos. Chem. Phys., https://doi.org/10.5194/acp-18-12391-2018, 2018.
Tan, Z., Lu, K., Jiang, M., Su, R., Wang, H., Lou, S., Fu, Q., Zhai, C., Tan, Q., Yue, D., Chen, D., Wang, Z., Xie, S., Zeng, L., and Zhang, Y.: Daytime atmospheric oxidation capacity in four Chinese megacities during the photochemically polluted season: A case study based on box model simulation, Atmos. Chem. Phys., 19, 3493–3513, https://doi.org/10.5194/acp-19-3493-2019, 2019.
Wang, M., Chen, D., Xiao, M., Ye, Q., Stolzenburg, D., Hofbauer, V., Ye, P., Vogel, A. L., Mauldin, R. L., Amorim, A., Baccarini, A., Baumgartner, B., Brilke, S., Dada, L., Dias, A., Duplissy, J., Finkenzeller, H., Garmash, O., He, X. C., Hoyle, C. R., Kim, C., Kvashnin, A., Lehtipalo, K., Fischer, L., Molteni, U., Petäjä, T., Pospisilova, V., Quéléver, L. L. J., Rissanen, M., Simon, M., Tauber, C., Tomé, A., Wagner, A. C., Weitz, L., Volkamer, R., Winkler, P. M., Kirkby, J., Worsnop, D. R., Kulmala, M., Baltensperger, U., Dommen, J., El-Haddad, I., and Donahue, N. M.: Photo-oxidation of Aromatic Hydrocarbons Produces Low-Volatility Organic Compounds, Environ. Sci. Technol., 54, 7911–7921, https://doi.org/10.1021/acs.est.0c02100, 2020a.
Wang, S., Wu, R., Berndt, T., Ehn, M., and Wang, L.: Formation of Highly Oxidized Radicals and Multifunctional Products from the Atmospheric Oxidation of Alkylbenzenes, Environ. Sci. Technol., 51, 8442–8449, https://doi.org/10.1021/acs.est.7b02374, 2017.
Wang, Y., Mehra, A., Krechmer, J. E., Yang, G., Hu, X., Lu, Y., Lambe, A., Canagaratna, M., Chen, J., Worsnop, D., Coe, H., and Wang, L.: Oxygenated products formed from OH-initiated reactions of trimethylbenzene: autoxidation and accretion, Atmos. Chem. Phys., 20, 9563–9579, https://doi.org/10.5194/acp-20-9563-2020, 2020b.
Watne, Å. K., Psichoudaki, M., Ljungström, E., Le Breton, M., Hallquist, M., Jerksjö, M., Fallgren, H., Jutterström, S., and Hallquist, Å. M.: Fresh and Oxidized Emissions from In-Use Transit Buses Running on Diesel, Biodiesel, and CNG, Environ. Sci. Technol., 52, 7720–7728, https://doi.org/10.1021/acs.est.8b01394, 2018.
Whalley, L. K., Slater, E. J., Woodward-Massey, R., Ye, C., Lee, J. D., Squires, F., Hopkins, J. R., Dunmore, R. E., Shaw, M., Hamilton, J. F., Lewis, A. C., Mehra, A., Worrall, S. D., Bacak, A., Bannan, T. J., Coe, H., Percival, C. J., Ouyang, B., Jones, R. L., Crilley, L. R., Kramer, L. J., Bloss, W. J., Vu, T., Kotthaus, S., Grimmond, S., Sun, Y., Xu, W., Yue, S., Ren, L., Joe, W., Nicholas Hewitt, C., Wang, X., Fu, P., and Heard, D. E.: Evaluating the sensitivity of radical chemistry and ozone formation to ambient VOCs and NOxin Beijing,

Atmos. Chem. Phys., 21, 2125–2147, https://doi.org/10.5194/acp-21-2125-2021, 2021.
Yang, C., Yao, N., Xu, L., Chen, G., Wang, Y., Fan, X., Zhou, P., Clusius, P., Tham, Y. J., Lin, Z., Chen, Y., Li, M., Hong, Y., and Chen, J.: Molecular Composition of Anthropogenic Oxygenated Organic Molecules and Their Contribution to Organic Aerosol in a Coastal City, Environ. Sci. Technol., 57, 15956–15967, https://doi.org/10.1021/acs.est.3c03244, 2023.
Yao, L., Garmash, O., Bianchi, F., Zheng, J., Yan, C., Kontkanen, J., Junninen, H., Mazon, S. B., Ehn, M., Paasonen, P., Sipilä, M., Wang, M., Wang, X., Xiao, S., Chen, H., Lu, Y., Zhang, B., Wang, D., Fu, Q., Geng, F., Li, L., Wang, H., Qiao, L., Yang, X., Chen, J., Kerminen, V.-M., Petäjä, T., Worsnop, D. R., Kulmala, M., and Wang, L.: Atmospheric new particle formation from sulfuric acid and amines in a Chinese megacity, Science (80-.)., 361, 278–281, https://doi.org/10.1126/science.aao4839, 2018.